LUND UNIVERSITY

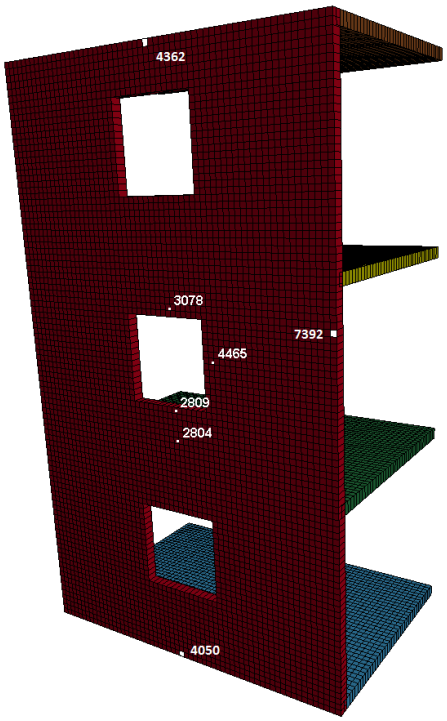

SIMULATIONS OF THE RESPONSE OF CONCRETE STRUCTURES SUBJECTED TO AIR BLASTS

PETER SVANTESSON

Structural Mechanics

Master's Dissertation

DEPARTMENT OF CONSTRUCTION SCIENCES

DIVISION OF STRUCTURAL MECHANICS

ISRN LUTVDG/TVSM--13/5193--SE (1-66) | ISSN 0281-6679

MASTER'S DISSERTATION

SIMULATIONS OF THE RESPONSE OF CONCRETE STRUCTURES SUBJECTED TO AIR BLASTS

PETER SVANTESSON

Supervisors: **PER-ERIK AUSTRELL**, Assoc. Professor; Div. of Structural Mechanics, LTH, Lund and **SAED MOUSAVI**, PhD; Swedish Defence Research Agency, FOI.

Examiner: **KENT PERSSON**, PhD; Div. of Structural Mechanics, LTH, Lund.

Printed by Media-Tryck LU, Lund, Sweden, November 2013 *(Pl)*.

For information, address:
Div. of Structural Mechanics, LTH, Lund University, Box 118, SE-221 00 Lund, Sweden.
Homepage: http://www.byggmek.lth.se

ABSTRACT

The response of concrete structures subjected to blast load can be studied numerically using commercial finite element programs. The complexity of reinforced concrete makes modeling and simulation of large structures time and computer power consuming. Consequently, The Swedish Defense Research Agency, FOI, has an interest in finding a fast and numerically efficient model to study this response to a reasonable cost.

A FOI report investigates the possibility to use a simplified numerical model of reinforced concrete slabs to simulate the response from blast loads and quasi static loads. The model is based on three-dimensional solid elements and a combined concrete/steel material model. The results are compared to an experimental study.

This thesis introduces a further simplified model of the concrete slabs based on shell element formulation. A combined concrete/steel material model for shell and beam type elements is used. Layered design is used where the reinforcement is smeared over a layer corresponding to the allocation of the longitudinal bars. The introduced model is used to simulate a part of a multi-story building subjected to blast load. The results are compared to existing results from experiments performed on structures in 1:4 scale.

Simulations of the slabs using a shell element formulated model shows that the shell model can predict the response of a blast load with similar accuracy as the solid element formulated model. For two different charge weights, the maximum deflection is however 1.6 and 2.2 times bigger than the results from experiments. The shell element formulated slab predicts a fair response from quasi static loads, but not with the same accuracy as the solid element slab.

Simulations of the multi-story building shows a façade mean deflection 3.0 times bigger than the experimental results. Additionally, the deflection remains permanent as opposed to the experiment where the permanent deformation is close to zero.

The introduced model is deemed to be able to constitute a base for further studies of simulations with shell element formulated concrete structures. A first step would be to introduce a more correct blast load for a better evaluation of the response.

Key words: Load blast, reinforced concrete, structural response, finite element analysis, LS-DYNA, LOAD BLAST ENHANCED, shell element

SAMMANFATTNING

Responsen från en betongstruktur som utsätts för en luftstötvåg kan studeras numeriskt med hjälp av kommersiella finita element-program. Armerad betong är ett komplext material och modellering och simulering av stora betongstrukturer är krävande i tid och datorkraft. Totalförsvarets forskningsinstitut FOI har därför ett intresse av att finna en snabb och numeriskt effektiv modell för att kunna studera denna respons till en rimlig kostnad.

I en tidigare FOI-rapport undersöks möjligheten att använda en förenklad numerisk modell av betongplattor för att studera responsen från luftstötvåg och kvasi-statisk belastning. Modellen baseras på tredimensionella solida element och en materialmodell med kombinerad betong/stål. Resultaten jämförs med en experimentell studie.

Det här examensarbetet introducerar en ytterligare förenklad modell av betongplattorna baserad på skalelementformulering. En kombinerad materialmodell för betong och stål anpassad för skal- och balkelement används. Plattorna modelleras med en skiktad design där armeringsstålet smetas ut över ett lager som motsvarar de längsgående stängernas placering. Den introducerade modellen används för att simulera en del av en flervåningsbyggnad som utsätts för luftstötvåg. Resultaten från simuleringarna jämförs med resultat från tidigare genomförda experiment på betongstrukturer i skala 1:4.

Simulering av betongplattor med skalmodellen visar att denna kan förutsäga responsen från en luftstötvåg med liknande noggrannhet som modellen baserad på solida element. För två olika laddningsvikter är den maximala utböjningen dock 1.6 och 2.2 gånger större än vad experimenten visar. Den skalelementformulerade modellen kan inte förutsäga responsen från kvasi-statisk belastning med samma noggrannhet som den solidelementformulerade modellen.

Simulering av flervåningsbyggnaden visar på en utböjning av fasaden som i medelvärde är 3.0 gånger större än experimentella resultatet. Utböjningen förblir dessutom permanent till skillnad från experimentet där den permanenta deformationen är nära noll.

Den introducerade modellen bedöms kunna utgöra en grund för vidare studier av simulering med skalelementformulerade betongstrukturer. Ett första steg vore att introducera en mer korrekt trycklast för att bättre kunna utvärdera responsen.

Nyckelord: Luftstötvåg, armerad betong, strukturrespons, finita elementanalys, LS-DYNA, LOAD BLAST ENHANCED, skalelement

Contents

Preface

This work is a degree project in structural mechanics for engineers at Lund Institute of Technology. It was performed at the Swedish Defense Research Agency (FOI) between June and November 2013.

I would like to thank the personnel at FOI Grindsjön who welcomed me into the team and made my time there worthwhile, professionally as well as socially.

Especially I would like to thank Saed Mousavi, Sebastian Bernhardsson and Rickard Forsén at FOI for the help and support with my work.

Stockholm, November 2013

Peter Svantesson

1. Introduction

The Swedish Defense Research Agency, FOI, has an interest in studying the behavior of large concrete structures, e.g. multi-story buildings, subjected to the air blast from an explosive device. The unrealistic magnitude of full scale testing makes it necessary to study this interaction numerically using finite element analysis.

Finite element simulation of large structures consisting of complex materials, such as reinforced concrete, is time and computer power consuming. Therefore it is necessary to make simplifications in order to arrive at fast and numerically efficient models.

A series of experiments with slabs subjected to blast loads done at FOI have been compared with numerical simulations based on 3D solid elements. In this work, the results of these experiments and simulations have been compared with a simplified finite element model based on shell element formulation. The shell element formulated slab model has then been used to simulate a multi-story building subjected to blast load. Results have been compared to the results from scaled experiments.

1.1. Aim

The aim of this thesis is to introduce a simplified numerical model based on shell element formulation of a multi-story concrete building subjected to blast load using commercial finite element computer code.

The initial step is to find a reliable but simple and numerically efficient finite element model of reinforced concrete slabs subjected to quasi static load and blast load using shell element formulation.

1.2. Background theory

1.2.1. Explosions and blast effects

An open air explosion constitutes a compact high energy gas pushing the surrounding atmosphere away under high pressure (Johansson, 2002). This creates a supersonic blast wave moving from the center of the explosion. Behind the blast wave front is a region where pressure, temperature, density and speed of the air particles are severely higher than in the surrounding air. The energy decreases as the blast wave moves away from its source, relapsing the increased pressure, density and speed back to the original ambient state. The temperature, however, gains a certain increase because of the increased entropy from the blast wave. The increased pressure and relapse back to ambient pressure is called the positive phase and is followed by a negative phase, characterized by a pressure lower than the ambient, causing a reversal of the particle flow (Krauthammer, 2008).

How a blast wave affects the surroundings is primarily dependent on the released energy and distance from the explosion source. However, more detailed information is needed to describe the blast wave impact, why physical quantities such as pressure, impulse and duration are used. Generally speaking, an increasing amount of energy leads to higher pressure and greater specific impulse. Increasing distance leads to a decreasing pressure and impulse, whereas the duration increases (Johansson, 2002).

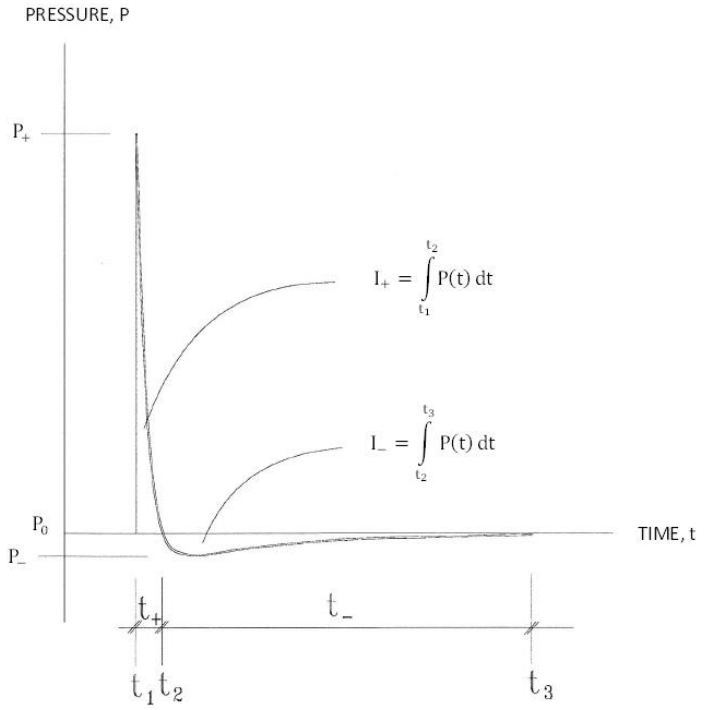

Figure 1.1. Time-pressure variation of an ideal blast wave. Based on FOI (2009).

The pressure-time relationship for an ideal blast wave is shown in Figure 1.1. The arrival of the blast wave at time t_1 causes the *peak pressure* P_+ to arise very fast. The peak pressure decays and reaches ambient pressure P_0 at t_2 where the negative phase begins and reaches the amplitude P_-. The pressure then relapses to P_0 at time t_3. The specific impulse for the positive and negative phases respectively are defined as

$$I_+ = \int_{t_1}^{t_2} P(t)dt \tag{1.1}$$

$$I_- = \int_{t_2}^{t_3} P(t)dt \tag{1.2}$$

The total impulse is defined as

$$I_{tot} = \int_{t_1}^{t_3} P(t)dt \tag{1.3}$$

Figure 1.2 shows a schematic picture of a building subjected to a blast wave. According to Krauthammer (2008), the negative phase is not important in structural design contexts and is usually ignored.

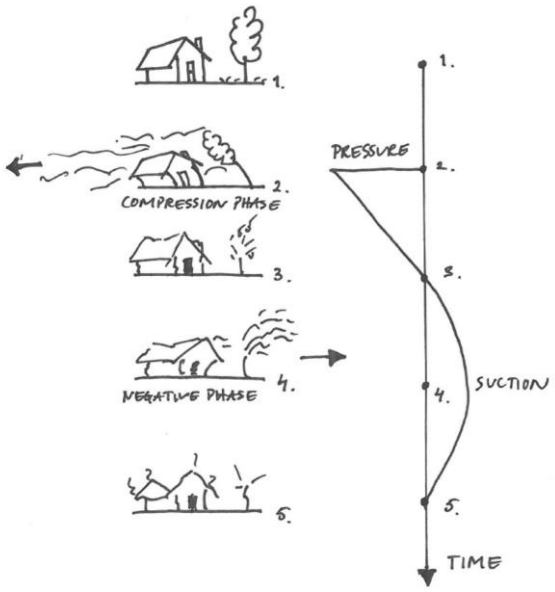

Figure 1.2. Schematic picture of building subjected to air blast showing the impact of positive and negative phases. Based on Johansson (2002).

If the wave encounters an obstacle that is not parallel to the direction of propagation, e.g. a wall or structure, a reflected pressure higher than the peak incident pressure is generated (Krauthammer, 2008). When an explosive device detonates on or close to the ground the gases are prevented from expanding downwards, causing an upward reflection, or mirroring, of the blast wave (FOI, 2009). Ideally, the energy of the reflected blast wave corresponds to

a charge weight twice the size of the charge weight in a free air detonation, as shown in Figure 1.3. Some of the energy is however absorbed into the ground which makes an increasing factor of 1.8 a good approximation.

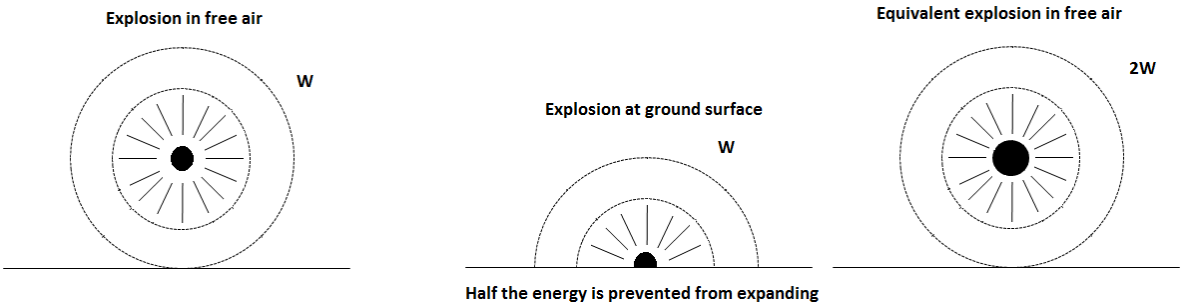

Figure 1.3. Mirroring of explosion at ground surface. Based on Johansson (2002).

1.2.2. Previous work on simulations of buildings subjected to blast load

Lucconi et al. (2003) emphasize two important features when performing computer blast resistance assessment of buildings. The first is the need for experimental validation. A lot of research has been done on structural elements and materials subjected to blast loads, however most of the full-scale results come from actual accidental explosions or terrorist attacks. The second is the problem that the computational cost makes it impracticable to make a realistic blast analysis of an actual building with all its details. A lot of assumptions and simplifications have to be done in order to perform the analysis. Many of them are related to the structural constituents' material properties, which have to be treated as homogenous with average properties.

In the paper *Analysis of building collapse under blast loads* (Luccioni, et al., 2004) a numerical simulation of the AMIA building collapse in Argentina 1994 is made using the finite element program AUTODYN. The AMIA building suffered a structural collapse as a consequence of a terrorist attack with a 400 kg TNT bomb. The AMIA buildings structural elements consisted of reinforced concrete columns, beams and slabs.

To model the reinforced concrete, Lucconi et al. (2003) use a homogenized elastoplastic material, similar to concrete material models, but with higher tension strength to take the reinforcement tension strength into account. Results show a good agreement between actual and simulated damage. The authors conclude that simplifying assumptions for the structure and materials are allowable for this kind of analysis and that this is the only way of successfully run a complete collapse analysis of an entire building.

Phuvoravan & Sotelino (2005) aims at developing a new finite element model for the nonlinear analysis of reinforced concrete slabs that is simple, easy to use and efficient, yet able to capture the effect of each individual reinforcement bar. It is concluded that there are two techniques for modeling reinforced concrete slabs: with discrete or layered modeling of reinforcement. Discrete modeling of the reinforcement is considered to provide a more realistic representation than the layered; however, it is more expensive in computational costs. Also, the model is more difficult and time consuming to construct. Layered modeling is on the other hand simple but can only represent highly reinforced concrete. Incorporation of bond slip can only be done artificially with the layered method.

Phuvoravan & Sotelino (2005) present a reinforced concrete slab model that combines four-node Kirchhoff shell elements for the concrete with two-node Euler beam elements for the reinforcement, implemented in the ABAQUS finite element software. The element is verified with experimental results and is shown to yield a good representation of the behavior of concrete slabs, especially for lightly reinforced ones.

Barmejo et al. (2011) use the finite element program LS-DYNA to simulate structural concrete columns, beams and slabs in a similar way; concrete shell elements together with steel beam elements. For the concrete modeling they use the LS-DYNA EC2 (*MAT_172) material model. The EC2 model can include reinforcement as a fraction of steel, which is used to model the transverse reinforcement as beams are used for the longitudinal reinforcement. The reinforcement steel material model is the piecewise linear plasticity (*MAT_024). Corresponding column, beam and slab elements are also constructed using continuum element models with the CSCM material model (*MAT_159) and beam element reinforcement. A quasi static bending and dynamic response comparison are performed between the two in order to calibrate the shell/beam structural elements. The shell/beam model is then used to evaluate the response of a frame-type building subjected to blast loading. It is concluded that the shell/beam model is accurate enough to provide the basis for a realistic simulation of the response of a full-scale building.

2. Method and material

The benchmark of this work is a FOI report by Bernhardsson & Forsén (2013) who investigates the possibility to study the response of reinforced concrete slabs subjected to quasi static loading and air blast loading from an explosion using simplified numerical simulations. A reproduction of Bernhardsson & Forsén's work using shell element formulation is done to evaluate the possibilities of further simplifications of reinforced concrete structure simulations.

Results are then used to simulate the response of a multi-story concrete building subjected to air blast load. The results of the multi-story building simulation are compared with existing results from experiments on concrete structures, described in 2.1.2.

The response is mainly investigated in terms of deformations or deflections as a function of time. Mechanisms for damage and/or collapse of the structures are not included in the models. Structures are modeled using shell element formulation and combined concrete/steel material models, i.e. no explicit formulations of the reinforcement bars are made. Only strict air blast load is taken into account and loads are applied using implemented functions. No simulations of actual blast and the following wave propagations are conducted.

2.1. Former work at FOI

2.1.1. Slabs subjected to blast and quasi static loads

In the report by Bernhardsson & Forsén (2013), simulations of concrete slabs subjected to blast and quasi static loading are performed and compared to former experimental studies presented in the report by Johansson (1978). Simulations are done with the general purpose finite element program LS-DYNA.

In the experimental study by Johansson (1978), simply supported, simple reinforced concrete slabs are subjected to quasi static load (four point bending) and blast load from TNT explosive charges. The slabs used for the computer simulated comparison are 2440x1230x153 mm and have a concrete compressive strength of 37 MPa and density of 2340 kg/m^3. The slab design can be seen in Figure 2.1. The measured stress-strain relationship of the reinforcement steel used by Johansson (1978) can be seen in Figure 2.2. Figure 2.2 also shows the stress-strain curve used in the simulations by Bernhardsson & Forsén (2013). The experimental setup for the four point bending experiment is shown in Figure 2.3.

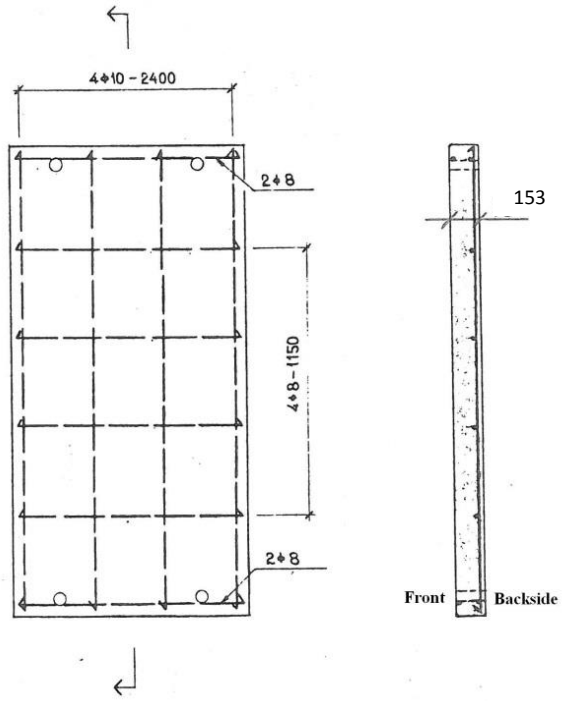

Figure 2.1. Design of slabs used in experimental study. From Johansson (1978).

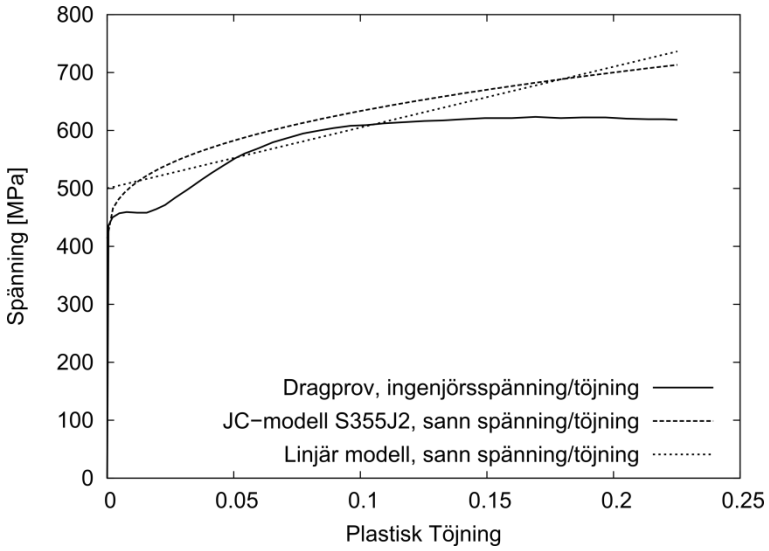

Figure 2.2. Steel stress as a function of plastic strain. Continuous line showing results of a tensile test of the reinforcement bars used by Johansson (1978). Light dotted line shows the Johnsson-Cook model used to adapt the linear model, shown as dark dotted line, used in the simulations. From Bernhardsson & Forsén (2013).

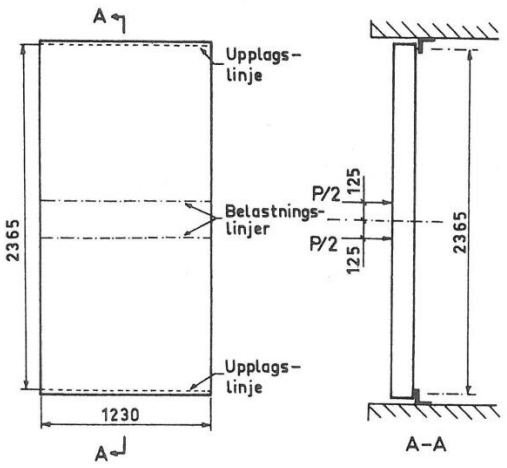

Figur 2.3. Setup used in quasi static load experiments, units in mm. The load P is applied along two lines in the middle of the slab. From Johansson (1978).

Bernhardsson and Forsén (2013) formulate the slabs with the combined reinforcement/concrete material model, `*MAT_16`/`*MAT_PSEUDO_TENSOR`, where the amount of reinforcement steel is defined as a fraction of the concrete. Eight-node cubic elements (hereafter referred to as *solid elements*) with a side length of 12.75 mm are used giving 12 through thickness element rows. The reinforcement is placed in the second lowermost row and has the equivalent amount of lengthwise reinforcement steel of 2 %. To avoid problems related to differences in impedance in different material properties, rows with a small amount of steel (0.05 %) are placed on either side. The slab is simply supported by rigid half cylindrical shell element supports. Half symmetry along the slab length is used in the simulations. The model is shown in Figure 2.4.

The blast load is applied using an automatic LS-DYNA function for pressure loads due to detonation of conventional explosives, `*LOAD_BLAST_ENHANCED`. Experimental data from two different trial setups were used from Johansson (1978), shown in Table 2.1. The quasi static loading is simulated with a linear prescribed motion of two rows of nodes corresponding to the load lines shown in Figure 2.3, with a total deformation of 250 mm during 10 seconds.

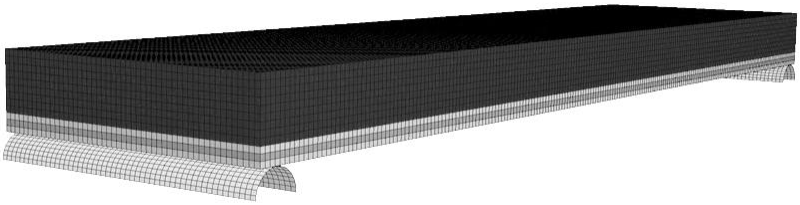

Figure 2.4. Model used by Bernhardsson & Forsén (2013).

Table 2.1. The two trial setups used. From Johansson (1978).

Trial	TNT weight (kg)	Charge distance (m)	Charge height (m)
P2b	48.2	8.80	1.32
P2d	50.0	5.40	0.85

Results are presented as support resultant force as a function of deflection for quasi static simulation, and as midpoint deflection as a function of time for the blast simulations. These are compared to the equivalent results from the experiments. Simulations with a smaller TNT weight of 20.0 kg are also done in both setups. Results are shown in Figures 2.5-7.

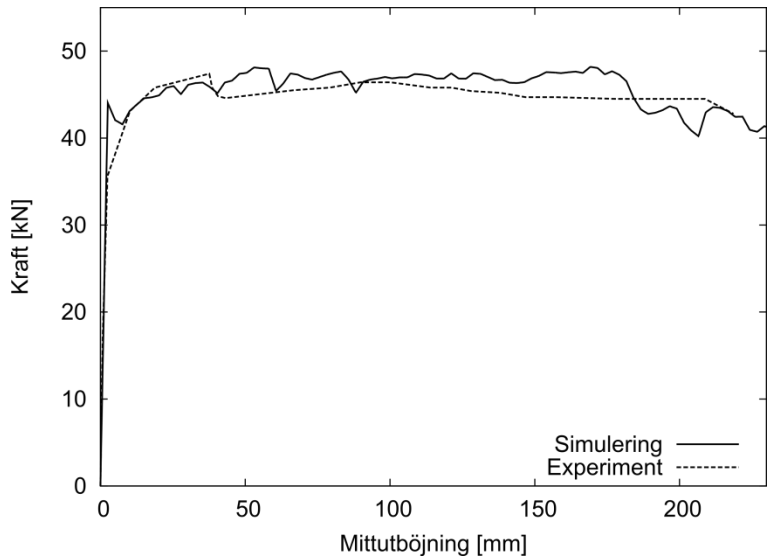

Figure 2.5. Force as a function of midpoint deflection comparing quasi static tests. Simulations by Bernhardsson & Forsén (continuous) and experimental results by Johansson (dotted). Note that simulated result is multiplied by two due to the half symmetry used. From Bernhardsson & Forsén (2013).

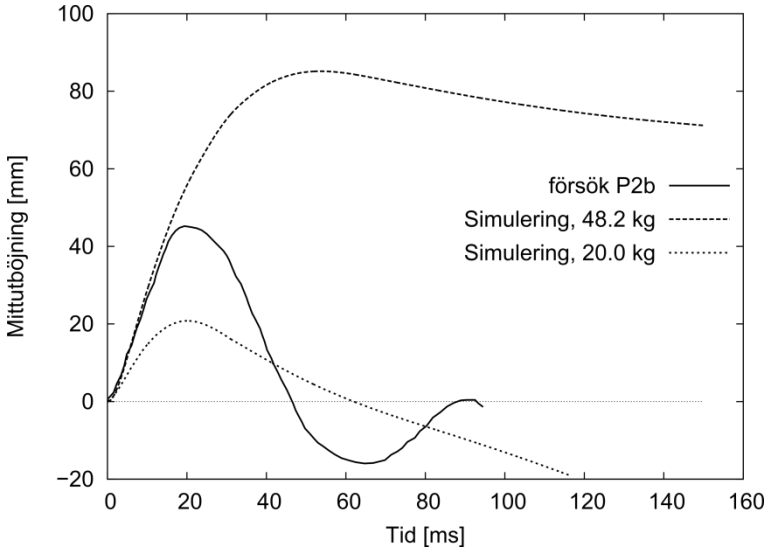

Figure 2.6. Midpoint deflection as a function of time comparing P2b blast load trials. Experimental results (continuous) and simulations with 48.2 kg charge weight (upper dotted) and 20.0 kg charge weight (lower dotted). From Bernhardsson & Forsén (2013).

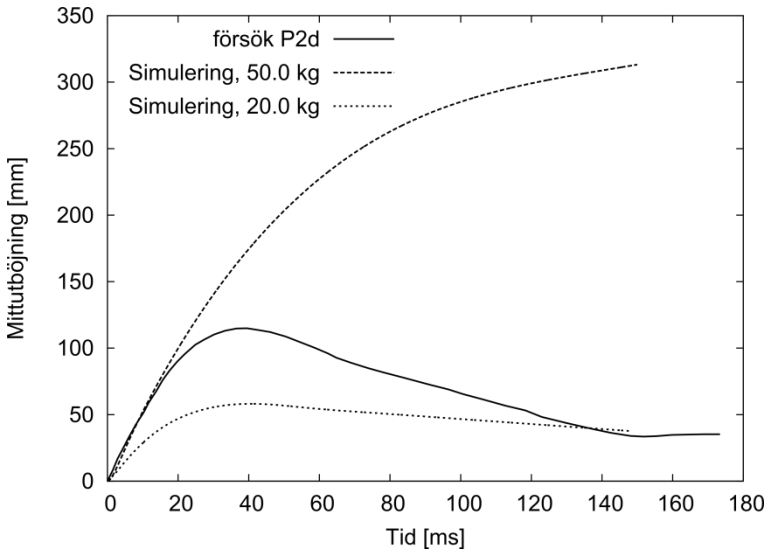

Figur 2.7. Midpoint deflection as a function of time comparing P2d blast load trials. Experimental results (continuous) and simulations with 50.0 kg charge weight (upper dotted) and 20.0 kg charge weight (lower dotted). From Bernhardsson & Forsén (2013).

The *LOAD_BLAST_ENHANCED (LBE) function is found to be a good and effective way of applying a blast load, especially if the structure design is complicated (Bernhardsson & Forsén, 2013). However, LBE underestimates the negative phase of the blast wave which can cause an overestimated structural response. The lower charge weight of 20 kg results in a lower peak pressure than in the experiments, but has an equivalent total impulse. It is recommended that this is considered in future work and alternate ways of applying the load where the negative phase is defined should be investigated.

The simulations show, that simplified concrete models with smeared reinforcement have a high quality in ability to predict a response close to experimental results, especially for quasi static loading. Because of the difficulties in applying the correct impulse, it is not possible to draw definite conclusions regarding the possibility to reproduce the deflection. The simulated response points towards the possibility of reproducing the correct response using a simplified concrete model. However, this must be studied further.

Results, especially from the quasi static simulation, are deemed adequate to constitute a base for work on further simplifications of the concrete modeling (Bernhardsson & Forsén, 2013).

2.1.2. Structures subjected to blast load

In a FOA (former FOI) report by Edin & Forsén (1991), a series of experiments are performed to determine the damages on a concrete multi-story building subjected to blast load from a 250 kg general-purpose bomb. Experiments are done with one fourth scale reinforced concrete structures simulating the external wall of a three story building with connecting floor slabs. A weight (400 or 800 kg) on top of the facade simulates mass load from above stories. The external wall is subjected to a blast load from a 2.1 kg spherical charge, equivalent to one fourth scale of the approximate 134 kg charge in a 250 kg general purpose bomb. The charge is placed facing the midpoint of the façade with distances of 0.7 to 4.5 m. The general design of the structure is shown in Figure 2.8. Two different reinforcement design setups are used, light and heavy. A detailed drawing showing the reinforcement design of the type 2 structure (heavily reinforced) is shown in Appendix F. The reinforcement steel used has a yield stress of 450 MPa and ultimate stress of 790 MPa at 23 % strain. The concrete has a compressive strength of 49 MPa and a density of 2150 kg/m^3.

Applied pressure, wall deflection and forces are measured at several points. The experimental setup can be seen in Figure 2.9, showing locations of displacement, pressure and force sensors.

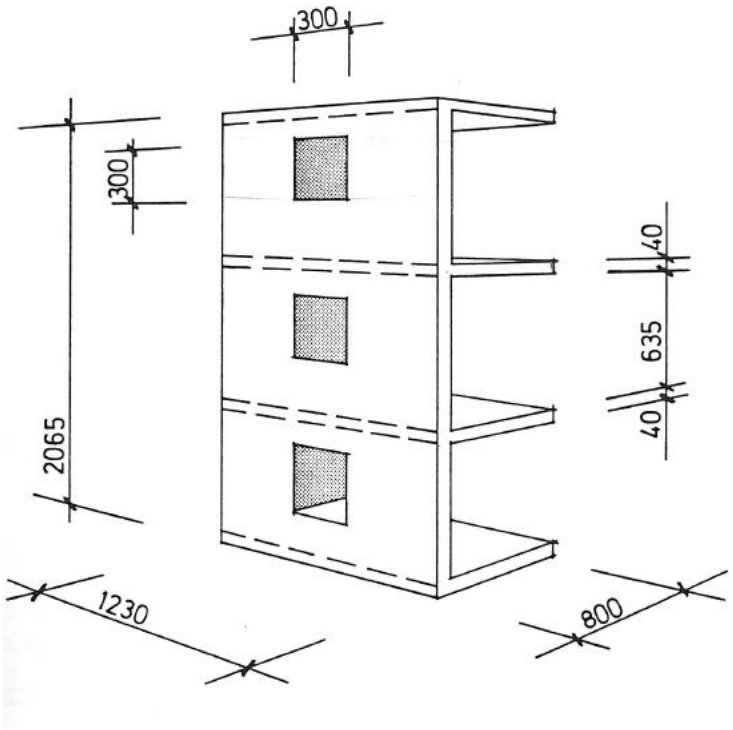

Figure 2.8. Design of the external wall, length units in mm. From Edin & Forsén (1991).

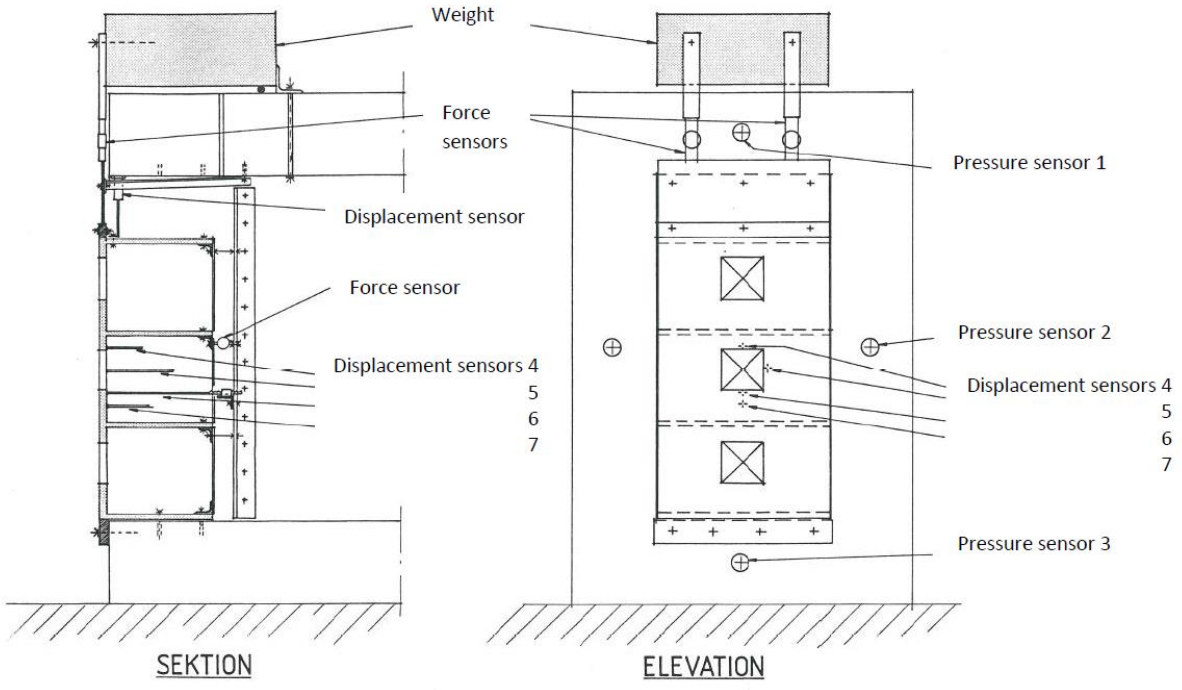

Figure 2.9. Experimental setup. Four displacement sensors are set around the second window. Force sensors are set on the third floor slab and on top of the façade wall. Three pressure sensors are set in the rig above, beneath and on the side of the façade wall.

2.2. Numerical simulations

The general purpose finite element program LS-DYNA is used for simulations. LS-DYNA is capable of handling nonlinear and transient dynamic analysis. The main solution method is explicit time integration with the possibility of implicit analysis (LSTC, 2013c). LS-DYNA is entirely command line driven and runs with a single ASCII format input file. Input files can also be generated with the graphical pre- and post-processor LS-PREPOST.

LS-DYNA features a great variety of material models. A compilation made by Bernhardsson (shown in Appendix B), shows that there are 31 different rock, soil and concrete material models available. Out of these there are seven including the possibility of mixed fraction of reinforcement. One is also compatible with shell element formulation; `*MAT_172`.

LS-DYNA material model 172, `*MAT_CONCRETE_EC2`, is for shell and Hughes-Liu beam elements only. It can represent reinforced concrete or plain concrete/plain reinforcement steel only (LSTC, 2013b). The position of the reinforcement steel cannot be explicitly defined within the concrete; hence the steel is evenly distributed, smeared, over the concrete cross section. The model features concrete crushing in compression, cracking in tension and reinforcement steel yield, hardening and failure.

Material data and equations describing the material behavior are taken from the European standard *Eurocode 2: Design of concrete structures – Part 1-2: General Rules – Structural fire design* (EN 1992-1-2:1995). If not defined, the material properties apply to 20°C (LSTC, 2013b). Updated concrete data from the 2004 release (EN 1992-1-2:2004) is available by setting concrete type 7 or 8 (`TYPEC 7` or `8`) (LSTC, 2013c).

2.2.1. *MAT_172 material model

The behavior of the material is controlled by user specified concrete compressive strength (stress), tensile stress to cause cracking and ultimate reinforcement (yield) stress (LSTC, 2013b). These three parameters combined with additional three; concrete mass density, steel elastic modulus and the reinforcement ratio, is enough to present an outline of a material model that should yield reasonable results.

The concrete is assumed to crack when in-plane principal tension stress reaches the specified maximum tensile strength (`FT`). A beginning crack growing to a fully open crack is by default assumed to have a bi-linear stress-strain curve where the parameter `ECUTEN` is strain to fully open crack (default value 0.0025). A simple linear relationship can be used by defining stress-strain slope value `ESOFT`. Concrete tensile behavior is shown in Figure 2.10.

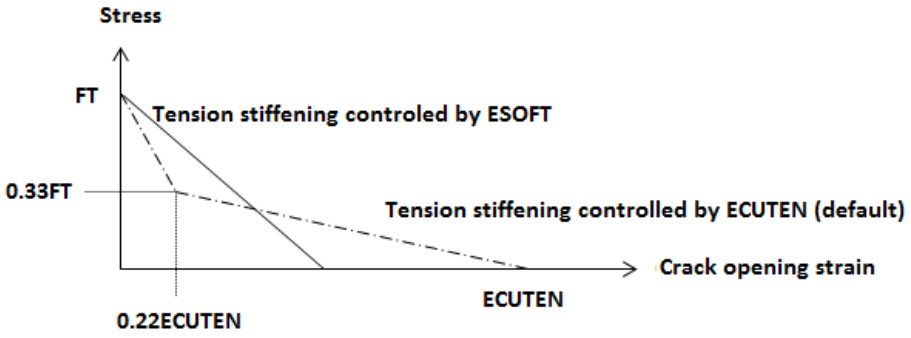

Figure 2.10. Tensile behavior of concrete in MAT_172. Based on LSTC (2013b).

A crack can open and close repeatedly. Concrete with closed cracks handles compressive stress according to the compressive stress-strain curve given by constitutive parameters.

The initial elastic modulus is defined as

$$E = \frac{3FC}{2\varepsilon_{c1}} \tag{2.1}$$

which is followed by the compressive stress-strain relationship defined as

$$Stress = \frac{3\varepsilon FC}{\varepsilon_{c1}\left(2+\left(\frac{\varepsilon}{\varepsilon_{c1}}\right)^3\right)} \tag{2.2}$$

where ε_{c1} is the ultimate strain where the ultimate compressive strength FC is met. At FC, stress decreases linearly until reaching zero at ε_{cu} (default set to 0.02). The overall concrete stress-strain relationship in tension and compression can be seen in Figure 2.11.

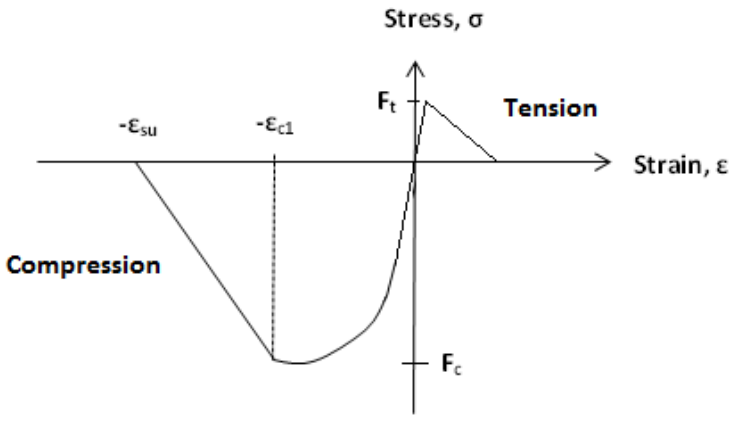

Figure 2.11. Concrete stress-strain curve in MAT_172. Based on LSTC (2013b).

The stress/strain relationship for reinforcement steel according to Eurocode 2 is shown in Figure 2.12.

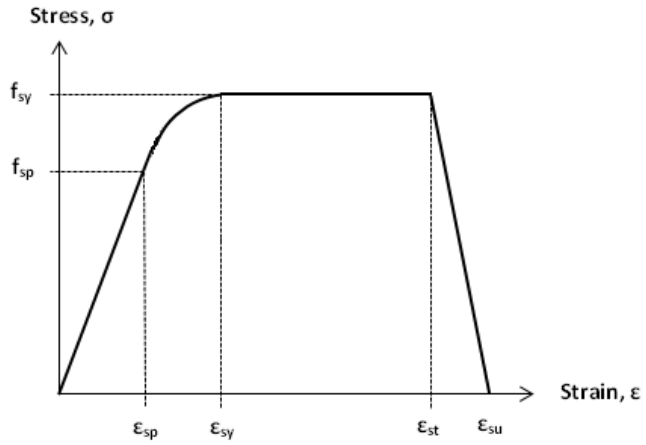

Figure 2.12. Steel stress-strain curve. Based on Eurocode 2.

The stress curve transition from elastic to plastic behavior ($\varepsilon_{sp} \leq \varepsilon \leq \varepsilon_{sy}$) is described as

$$\sigma = f_{sp} - c + (b/a)\left[a^2 - (\varepsilon_{sy} - \varepsilon)^2\right]^{0.5} \tag{2.3}$$

and the he initial tangent modulus

$$E = \frac{b(\varepsilon_{sy} - \varepsilon)}{a\left[(a^2 - (\varepsilon - \varepsilon_{sy})^2\right]^{0.5}} \tag{2.4}$$

Where

$$a^2 = \left(\varepsilon_{sy} - \varepsilon_{sp}\right)\left(\varepsilon_{sy} - \varepsilon_{sp} + \frac{c}{E_s}\right) \tag{2.5}$$

$$b^2 = c\left(\varepsilon_{sy} - \varepsilon_{sp}\right)E_s + c^2 \tag{2.6}$$

$$c = \frac{(f_{sy} - f_{sp})^2}{(\varepsilon_{sy} - \varepsilon_{sp})E_s - 2(f_{sy} - f_{sp})} \tag{2.7}$$

Strain parametres are defined as

$$\varepsilon_{sp} = \frac{f_{sp}}{E_s} \qquad \varepsilon_{sy} = 0.02 \quad \varepsilon_{st} = 0.15 \quad \varepsilon_{su} = 0.20 \tag{2.8}$$

`*MAT_CONCRETE_EC2` is also included with the possibility to override the Eurocode 2 stress-strain curve by setting type of reinforment to 5 (`TYPER = 5`) and defing a loadcurve (`LCRSU` refering to a curve defined by `*DEFINE_CURVE`). The yield stress is then given by

$$SUREINF \cdot f(\varepsilon_p) \tag{2.9}$$

where $f(\varepsilon_p)$ is the loadcurve value at the current plastic strain (LSTC, 2013b).

2.2.2. *PART_COMPOSITE and *LOAD_BLAST_ENHANCED

*PART_COMPOSITE is a simplified LS-DYNA function for defining layered composite material models using shell elements (LSTC, 2013a). Every element through thickness integration point is prescribed with a separate thickness and material, creating a composite with a total thickness equal to the sum of the integration point thicknesses. By combining different materials it is e.g. possible to define a concrete slab with the reinforcement concentrated to a certain layer or layers through the thickness. *PART_COMPOSITE also includes the same variables as *SECTION_SHELL which is an input card normally used to define the formulation, integration rule, nodal thickness and cross sectional properties for shell elements (LSTC, 2013a).

*LOAD_BLAST_ENHANCED (LBE) is an input function for applying blast load based on empirical data from the program Conventional Weapons Effects (ConWep). ConWep contains a collection of conventional weapons effects calculations where maximum pressure, impulse and duration as a function of scaled distance for TNT have been measured (Bernhardsson & Forsén, 2013). ConWep is intended for design and analysis of protective structures subjected to the effects of conventional weapons (Hyde, 1992). The only mandatory input parameters in LBE are the equivalent TNT charge weight (m), location of charge center (xbo, ybo and zbo) and a unique blast ID (bid). The blast load from the TNT is applied to a defined segment (element or set of elements in the mesh, defined by another mandatory function: *LOAD_BLAST_SEGMENT_SET) and the pressure on each element is defined by the formula

$$P(t) = P_1(1 + cos\theta - 2cos^2\theta) + P_R cos^2\theta \qquad (2.10)$$

where P_1 is the incident pressure, P_R is the reflected pressure and θ is the angle of approach. Perpendicular approach ($\theta = 0°$) means an applied pressure equal to the reflected pressure and parallel approach ($\theta = 90°$) means no enhanced pressure. If $\theta > 90°$ the applied pressure is set to the approaching pressure (Bernhardsson & Forsén, 2013). The type of blast source (BLAST) is alternatively defined as *hemispherical surface burst* (BLAST = 1), where the charge is located on or very near the ground surface, *spherical air burst* (BLAST = 2), with no amplification of the initial shock wave due to interaction with the ground surface, *air burst* (BLAST = 3) from moving non spherical warhead or *air burst with ground reflection* (BLAST = 4; valid for a certain range of scaled height of burst) (LSTC, 2013a). The treatment of the negative phase is either ignored (NEGPHS = 1) or included (NEGPHS = 0).

2.2.3. Slab simulation

With a mesh element size the same as used by Bernhardsson & Forsén (2013), 12.75 mm, the slab has a total of 10353 elements. A more course mesh with 2652 elements is also used. The *PART_COMPOSITE function is used with 12 through thickness integrations points (NIP) with reinforcement steel fraction in the second lowermost layer. This gives the same reinforcement steel lever as the solid slab by Bernhardsson & Forsén (2013).

Material model *MAT_EC2 is used with one setup including steel for the reinforcement layer and one without steel for the other layers. The input variables for the concrete are density, RO = 2340 kg/m3, compressive strength, FC = 30 MPa and tensile strength to cause cracking, FT = 3.8 MPa (tensile strength concrete C30, (Isaksson & Mårtensson, 2010)). Reinforcement input variables are Young's modulus, YMREINF = 200 GPa, Poissons ratio, PRRINF = 0.3, yield stress, SUREINF = 500 MPa and amount of reinforcement steel, FRACRX = 0.01 and FRACRY = 0.02. A complete description of the *MAT_172 variables is shown in Appendix D. Simulations are run using the default steel yield curve as well as the one with tension stiffening used by Bernhardsson & Forsén (2013), shown in Figure 2.2. Maximum steel stress is 731 MPa (1.462*SUREINF) at strain 0.22 (ε_{st}). The stress is assumed to decrease linearly to zero at ultimate strain (ε_{su}) 0.27.

The different setups of the quasi static simulations are shown in Table 2.2. The LS-DYNA ASCII code for simulation QS2 is shown in Appendix C.

Table 2.2. Shell slab configurations used for quasi static load simulations.

Name	QS1	QS2	QS3
Number of elements	2652	2652	10353
Steel yield curve	Default	Stiffening	Stiffening

Simulations are done with explicit time step analysis were the program determines the initial time step size. Simulations are done with a deflection speed of 25 mm per second to a total deformation of 250 mm.

For blast load simulations, the same configurations as in the quasi static simulations are used. The configurations are shown in Table 2.3. The TNT load is placed according to Table 2.1. Simulations are run 150 ms. Both P2b and P2d simulations are also conducted with a TNT load of 20 kg. The LS-DYNA ASCII code for LB1 is shown in Appendix E.

Table 2.3. Shell slab configurations used for blast load simulations.

Name	LB1	LB2	LB3
Number of elements	2652	2652	10353
Steel yield curve	Stiffening	Default	Stiffening
P2b charge weight (kg)	48.2 and 20.0	20.0	48.2 and 20.0
P2d charge weight (kg)	50.0 and 20.0	-	50.0 and 20.0

2.2.4. Structure simulation

The complete mesh model of the building wall is shown in Figure 2.13, showing the nodes used for measuring deflection (nodes 2804, 2809, 4465 and 3078) and segments used for measuring applied pressure (segments 4050, 7392 and 4362). These segments are for convenient reasons placed on the actual mesh whereas they are placed in the setup rig in the experimental study. The mesh element size is 20 mm.

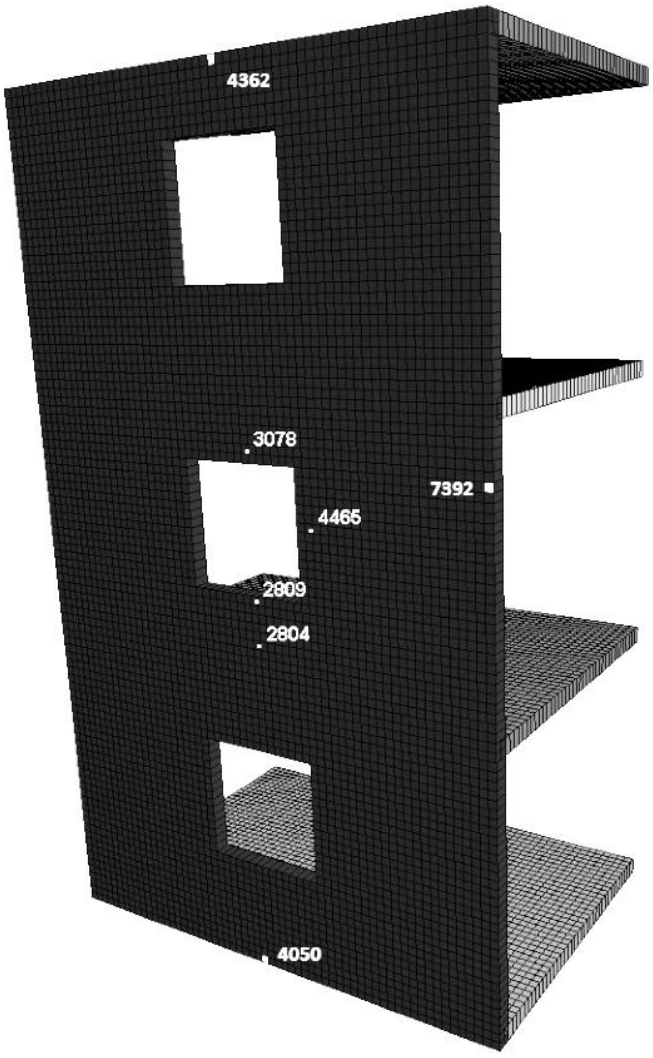

Figure 2.13. External wall mesh showing nodes and segments used for measuring deformation and applied pressure.

Simulations are compared with experiment number 480 which is heavily reinforced and use the 800 kg weight. The charge distance is 2.1 m.

*PART_COMPOSITE is used with a layer thickness of 4 mm, i.e. a total of 10 through thickness integration points are used. Reinforcement is placed in the second lowermost/topmost layers, giving a 4 mm concrete protection layer as in the actual structure. This gives a steel lever,

$$d_{simulation} = 40 - \left(4 + \frac{4}{2}\right) = 34.00\ mm\ . \quad (2.11)$$

Reinforcement steel with diameter 2.5 mm gives the experimental steel lever,

$$d_{experiment} = 40 - \left(4 + \frac{2.5}{2}\right) = 34.75\ mm. \quad (2.12)$$

Based on the detailed reinforcement drafting (Appendix F), steel fraction for a 4 mm layer is calculated, shown in Table 2.4.

Table 2.4. Calculated reinforcement steel fraction in a 4 mm layer. x, y and z-directions corresponds to the structure width, depth and height respectively.

Façade (front & back)	x-direction	z-direction
	0.015	0.012
Floor slab (bottom only)	x-direction	y-direction
	0.015	0.016

Façade to slab contacts are modeled with the *CONTACT_TIED_SHELL_EDGE_TO_SURFACE_OFFSET function, giving moment stiff connections. This function allows for an offset distance to be set due to the shell thickness. The back side of the structure have a joint type boundary with nodes locked in x, y, and z, but no rotational constraints. The lowermost nodes of the structure are constrained to move in all directions. The topmost row of nodes (64 nodes) on the façade element is set with *LOAD_NODE_SET, with nodal load equivalent to the 800 kg weight load on top of the structure.

This nodal load is calculated as

$$load_{800} = \frac{800 \cdot 9.81}{64} = 0.12\ kN/node \tag{2.13}$$

where 9.81 is the gravitational acceleration in m/s^2. The whole structure is subjected to the gravitational force through functions `*LOAD_BODY_Z` and `*LOAD_BODY_PARTS`. Two different blast modes are used with the `LBE`, *hemispherical surface burst* (`BLAST` = 1) and *spherical air burst* (`BLAST` = 2). A total of three setups are used, F1 with 2.1 kg TNT load using BLAST = 1, F2 with 2.1 kg, BLAST = 2 and F3 with 1.0 kg, BLAST = 2. All simulations are run with a total time of 50 ms. The LS-DYNA ASCII code is shown in Appendix G.

3. Results

3.1. Slabs

In the quasi static simulations, the deflection is increased linearly from zero to 250 mm during 10 seconds. Results are presented as support reaction force as a function of time, comparing the shell formulated slabs to the solid slab by Bernhardsson & Forsén (2013).

Figure 3.1 shows results from shell formulated slab with 10353 elements and stiffening reinforcement steel yield curve (QS3) compared to the solid formulated slab. The shell slab presents a higher resultant force, indicating a higher flexural rigidity. The resultant force drops to zero (i.e. the slab loses flexural rigidity) after 8.5 seconds, which is equivalent to 212.5 mm deflection. This is because of the reinforcement steel reaching its ultimate strain.

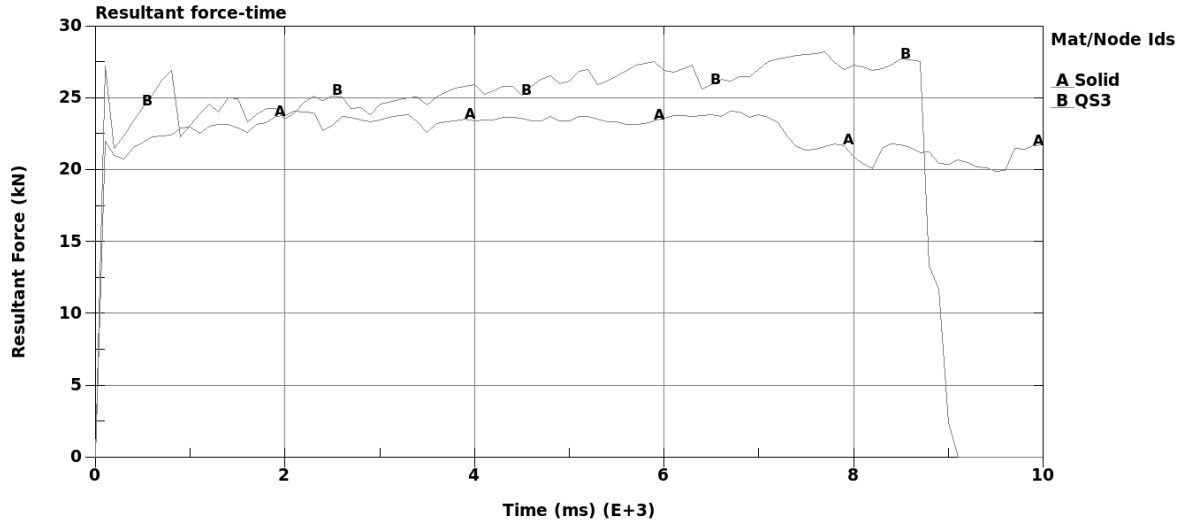

Figure 3.1. Resultant force as a function of time comparing solid slab from Bernhardsson & Forsén (2013) (A) to QS3 shell slab with 10353 elements and stiffening steel yield curve (B).

Figure 3.2 shows results from shell formulated slab with 2652 elements and stiffening reinforcement steel yield curve (QS2) compared to solid formulated slab. The resultant force has a repeated increasing-decreasing behavior and the slab loses flexural rigidity after about 4.5 seconds, equivalent to 112.5 mm. This is because of the reinforcement steel reaching its ultimate strain. The response up to 0.5 seconds is however more correspondent to the solid slab.

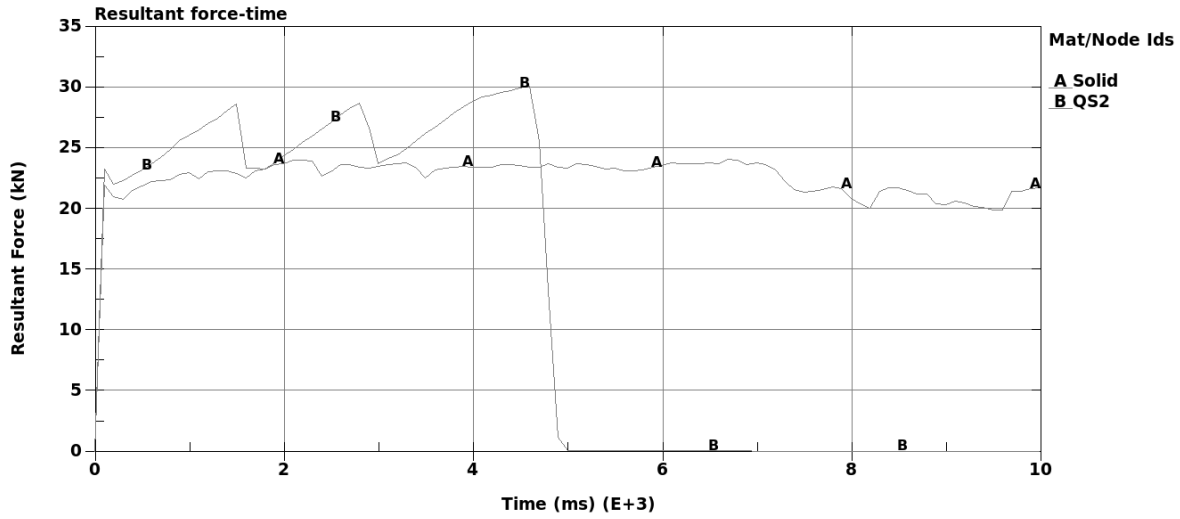

Figure 3.2. Resultant force as a function of time comparing solid slab from Bernhardsson & Forsén (2013) (A) to QS2 shell slab with 2652 elements and stiffening steel yield curve (B).

Figure 3.3 shows results from shell formulated slab with 2652 elements and the default `*MAT_172` steel yield curve (QS2) compared to the solid formulated slab. With this steel model the slab flexural rigidity is considerably lower.

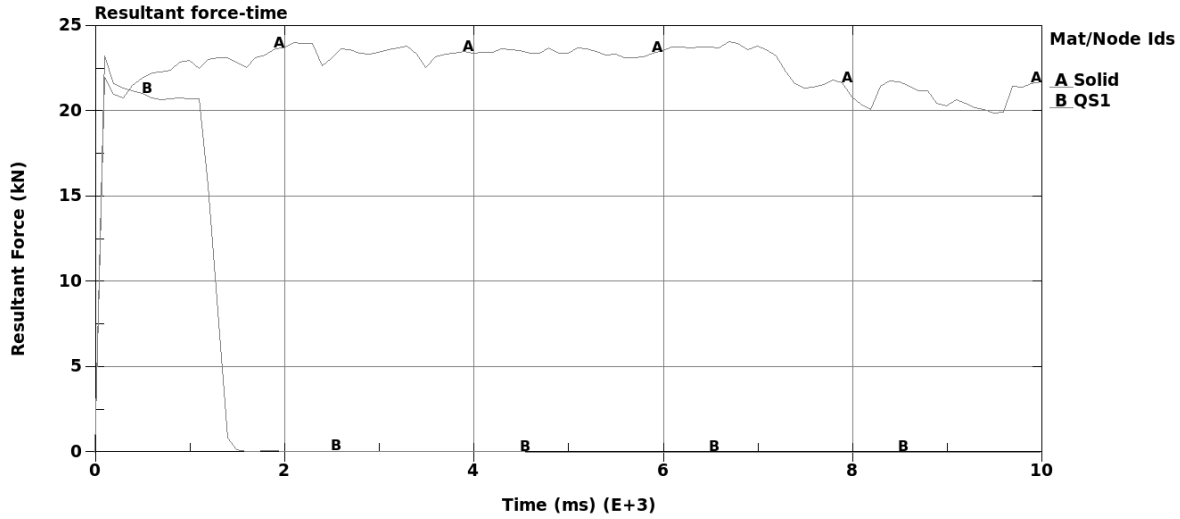

Figure 3.3. Resultant force as a function of time comparing solid slab from Bernhardsson & Forsén (A) to QS1 shell slab with 2652 elements and the default ideal plastic steel yield curve (B).

For the load blast simulations, results are presented as midpoint deflection as a function of time. The results are compared to equivalent results from the solid formulated slab by Bernhardsson & Forsén (2013).

Figure 3.4 shows results from simulation with P2d setup (48.2/20.0 kg charge weight, 8.8 m charge distance) using shell slab with 10353 elements and stiffening steel yield curve. The shell slab maximum deflection is smaller for the 48.2 kg load and bigger for the 20.0 kg load.

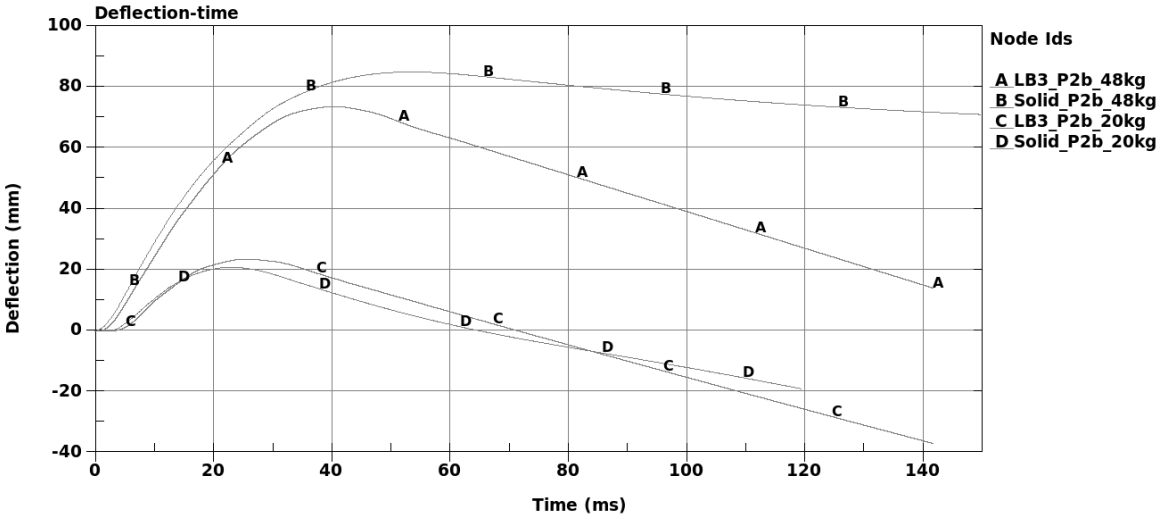

Figure 3.4. Midpoint deflection as a function of time for P2b simulations, comparing LB3 shell slab with 10353 elements (A and C) to solid slab (B and D).

Figure 3.5 shows the same comparison as Figure 3.4, but for P2d setup (50.0/20.0 kg charge weight, 5.4 m charge distance). The shell slab maximum deflection is smaller for the 50.0 kg load and bigger for the 20.0 kg load. For both P2b and P2d setups, the shell slabs show to have a faster reflection back towards its original zero-position.

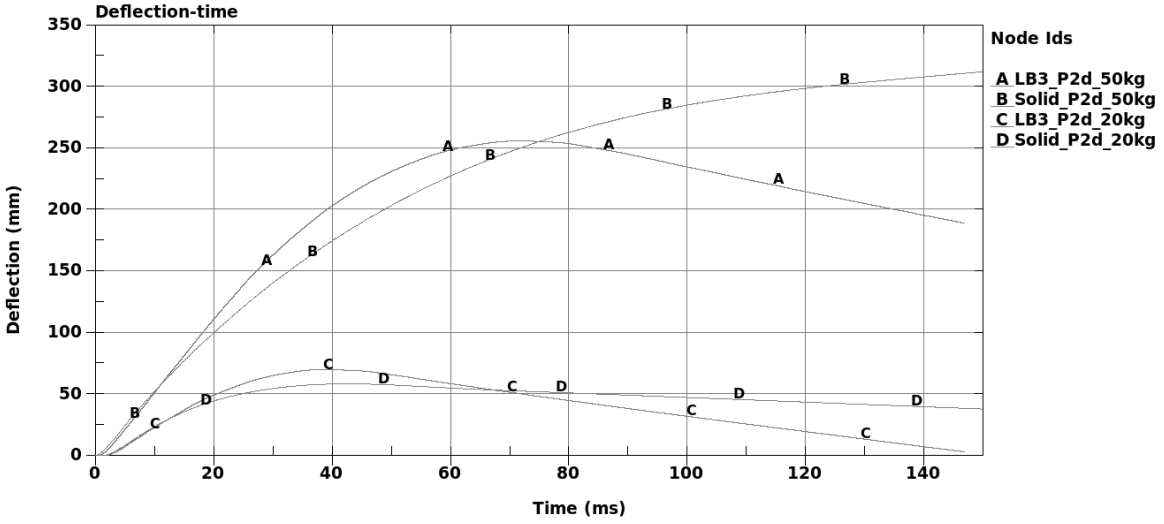

Figure 3.5. Midpoint deflection as a function of time for P2d simulations, comparing LB3 shell slab with 10353 elements (A and C) to solid slab (B and D).

Figure 3.6 shows a comparison between shell slabs using 10353 elements (LB3) and 2652 elements (LB1) for P2b setup. Differences in maximum deflection are small. Figure 3.7 show the same comparison for P2b setup. Results are close to identical.

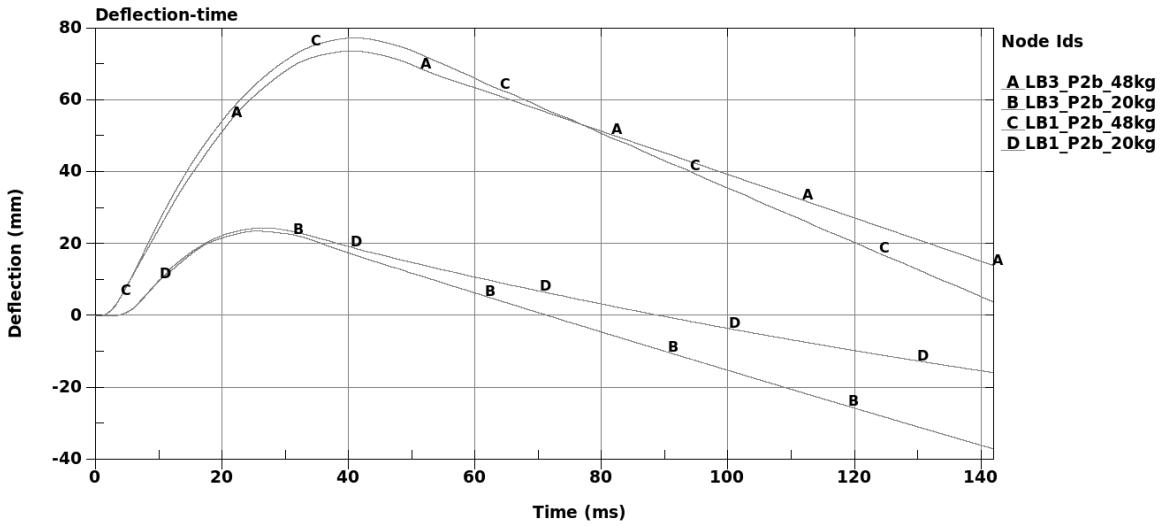

Figure 3.6. Midpoint deflection as a function of time for P2b simulations, comparing LB1 shell slab with 2652 elements (C and D) to LB3 shell slab with 10353 elements (A and B).

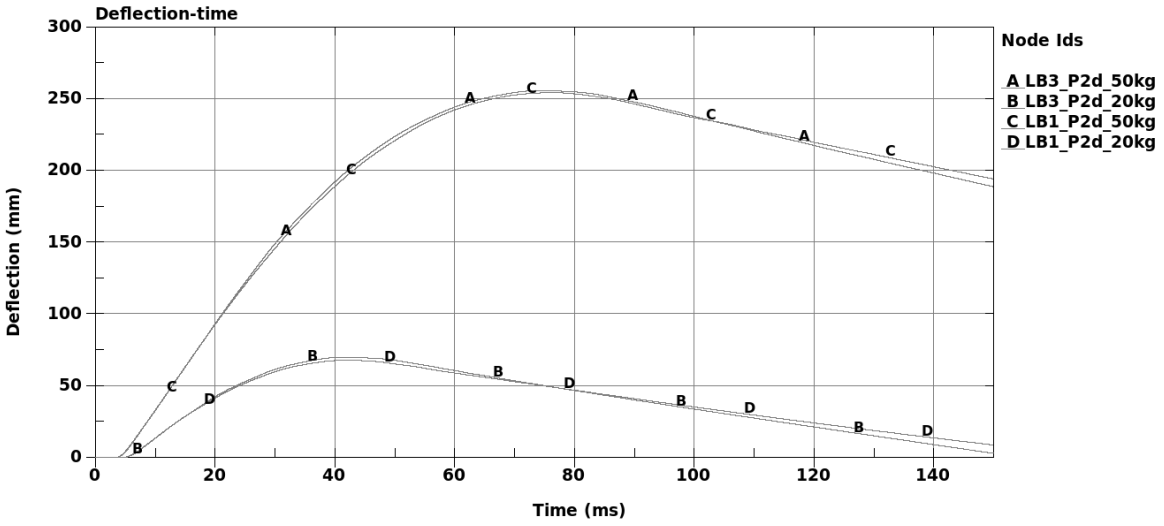

Figure 3.7. Midpoint deflection as a function of time for P2d simulations, comparing LB1 shell slab with 2652 elements (C and D) to LB3 shell slab with 10353 elements (A and B). Curves are close to identical.

Figure 3.8 shows midpoint deflection using slab with 2652 elements and the default `*MAT_172` steel yield curve (LB2). It is subjected to 20 kg with P2b setup which is the lightest blast load used in the simulations. The slab fails.

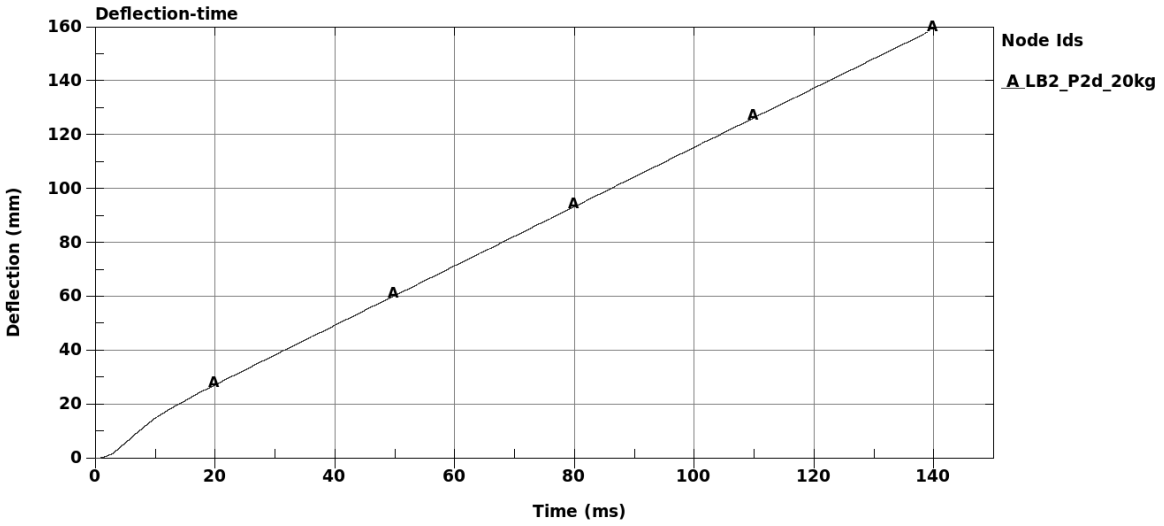

Figure 3.8. Midpoint deflection as a function of time for LB2 P2d 20.0 kg simulation. The slab fails.

3.2. Structure

Table 3.1 shows the positive and negative pressure, duration and impulse measured at three locations in Edin & Forsén (1991) experiment 480. It also shows the positive and negative pressure, duration and impulse applied by *LOAD_BLAST_ENHANCED for the three simulations F1, F2 and F3.

Table 3.1. Pressure, duration and impulse for simulations compared with data from experiment 480. F1 is 2.1 kg charge weight using BLAST = 1, F2 is 2.1 kg charge weight using BLAST = 2, F3 is 1.0 kg charge weight using BLAST = 2. Only peak pressures and total impulse are presented for F3.

Experiment	Pressure sensor	P_+ (kPa)	t_+ (ms)	I_+ (Pas)	P_- (kPa)	t_- (ms)	I_- (Pas)	I_{tot} (Pas)
480	1	776	2.19	355	38	27	216	139
	2	1020	1.85	384	62	25	194	190
	3	891	2.52	689	75	32	333	356
	Mean	-	-	-	-	-	-	228
Simulation	Segment	P_+ (kPa)	t_+ (ms)	I_+ (Pas)	P_- (kPa)	t_- (ms)	I_- (Pas)	I_{tot} (Pas)
F1	4362	1070	2.69	472	0.4	4.83	0.66	471
	7392	1320	2.74	507	0.2	4.95	0.24	507
	4050	1070	2.69	472	0.5	5.48	0.81	471
F2	4362	719	2.4	345	1.3	5.2	2.2	343
	7392	938	2.3	394	0.8	4.6	1.1	393
	4050	718	2.6	345	1.4	5.4	2.4	340
F3	4362	369	-	-	-	-	-	209
	7392	374	-	-	-	-	-	188
	4050	369	-	-	-	-	-	209
	Mean	-	-	-	-	-	-	202

Using BLAST = 1 (hemispherical surface burst) as in simulation F1, the applied positive peak pressures (P_+) are higher than in experiment 480. Using BLAST = 2 (spherical air burst) as in simulation F2, the positive peak pressures are comparable to the experiment.

As previously discussed, *LOAD_BLAST_ENHANCED underestimates the negative phase giving an overestimation of the total impulse. A charge weight of 1.0 kg and BLAST = 2, as used in simulation F3, approximately yields the same total impulse mean value (I_{tot}) as the experiment 480.

Figure 3.9 shows the time-pressure plot for segment 4362 subjected to 2.1 kg charge weight using `BLAST` = 2 (F2), illustrating the small negative phase.

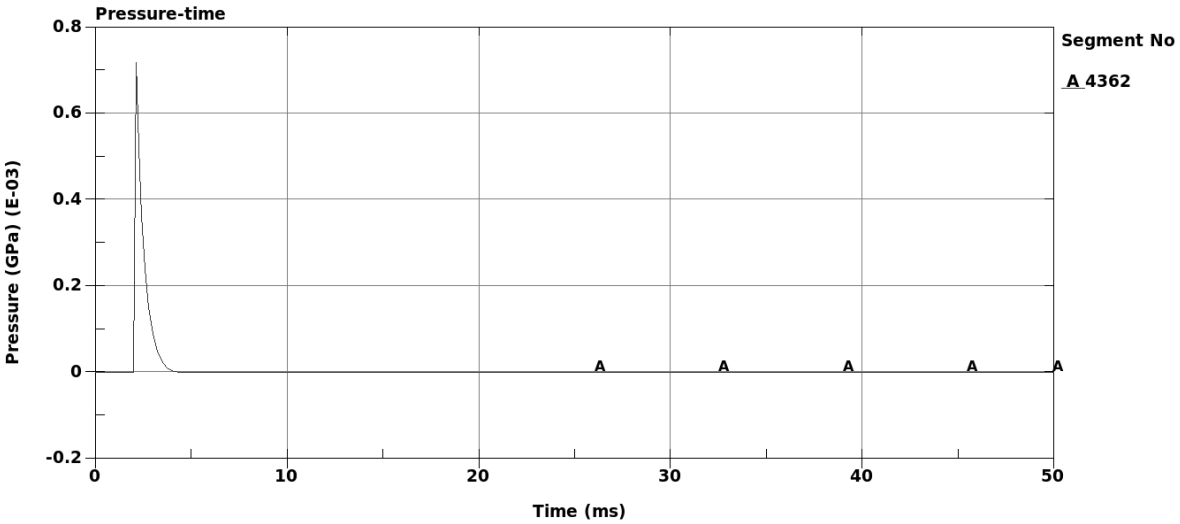

Figure 3.9. Time-pressure plot for F2 segment 4362. Negative phase is very small and cannot be distinguished from the plot.

Table 3.2 presents the measured displacements (deformations) and forces from experiment 480 and simulations F2 and F3.

Table 3.2. Results from simulations F2 and F3 compared to results from experiment 480. *Approximate values.

Experiment	Sensor	Max. horizontal def (mm)	Remaining horizontal def (mm)	Max. vertical def (mm)	Max. backw force, mean (kN)	Max. uppw force, mean (kN)
480	4	2.2	-	5.9	36.6	50.8
	5	4.4	0			
	6	5.1	0.5			
	7	3.5	0			
Simulation	Node					
F2	3078	7.0	7.0*	11.8	52.3	1.3
	4465	18.0	18.0*			
	2809	13.5	13.5*			
	2804	6.2	6.2*			
F3	3078	2.4	2.4*	3.5	68.8	1.2
	4465	6.0	6.0*			
	2809	5.2	5.2*			
	2804	2.6	2.6*			

Figure 3.10 shows deformation as a function of time from simulation F2 (2.1 kg, BLAST = 2). Deformations remain permanent after reaching peak value.

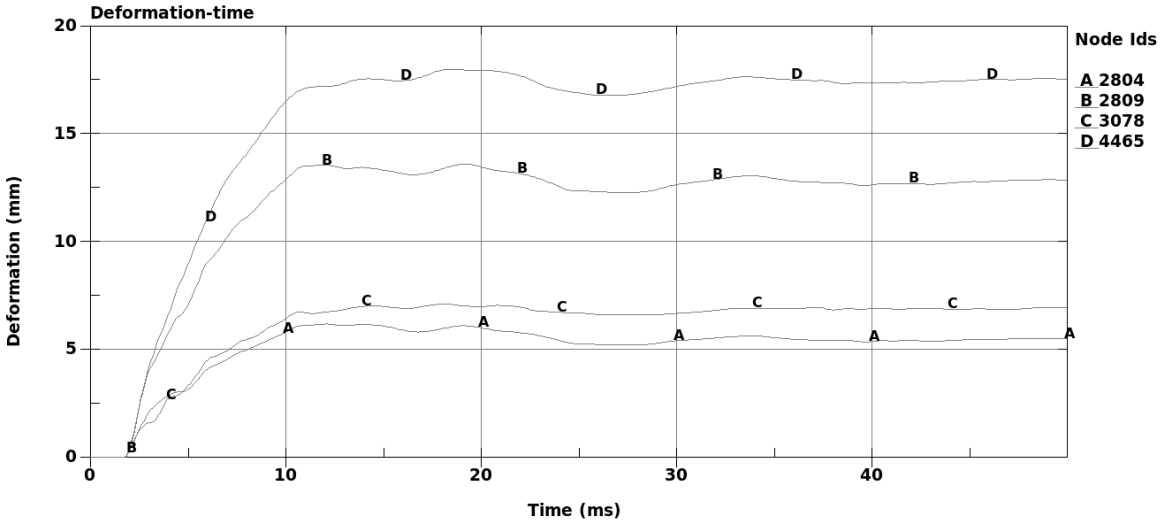

Figure 3.10. Deformation-time plot for F2. Deformation is permanent after reaching peak value.

To get a perception of the results from slab simulations compared to results from the wall simulation, the ratios between experimental and simulated responses (in terms of maximum deflection/deformation) are compared.

Table 3.3 shows ratios between simulated maximum deformation and experimental maximum deformation, comparing solid slab, shell slab (LB3) and building wall (simulation F2). Simulated building wall deformation is 3.0 times bigger than experimental deformation (mean value). Corresponding ratios for the shell slabs are between 1.6 and 2.2.

Table 3.3. Ratios between simulated and experimental maximum deformation, comparing solid slab, shell slab and external wall.

	$\frac{\text{Simulated deformation}}{\text{Experimental deformation}}$	
Slabs	P2b (48.2 kg)	P2d (50.0 kg)
Solid	1.9	2.7
Shell (10353 elements)	1.6	2.2
Wall, measured points	F2 (2.1 kg)	
3078	3.5	
4465	4.1	
2809	2.6	
2804	1.8	
Mean	3.0	

Table 3.4 shows the equivalent numbers from simulations with reduced charge weights (20.0 and 1.0 kg respectively). Slabs ratios are between 0.4 and 0.6 whereas the building wall has a ratio mean value of 1.1.

Table 3.4. Ratios between simulated and experimental maximum deformation with reduced charge weights, comparing solid slab, shell slab and external wall.

	$\frac{\text{Simulated deformation}}{\text{Experimental deformation}}$	
Slabs	P2b (20.0 kg)	P2d (20.0 kg)
Solid	0.4	0.5
Shell (10353 elements)	0.5	0.6
Wall, measured points	F3 (1.0 kg)	
3078	1.1	
4465	1.4	
2809	1.0	
2804	0.7	
Mean	1.1	

4. Discussion

The solid element formulated slab by Bernhardsson & Forsén (2013) is shown to be able to predict an accurate resultant force when simulated with quasi static load. Comparing these results from the solid element formulated slab to equivalent results from the shell element formulated slab, it is shown that the shell slab produces a less accurate prediction of the resultant force. Overriding the `*MAT_172` steel yield curve as done with QS3 and QS2 shell slabs, simulations show an overestimation of the slab flexural rigidity. Using the default steel curve as with QS1, the flexural rigidity is underestimated. The loss of flexural rigidity is as mentioned because of the steel reaching its ultimate strain and is a consequence of the deformation appearing very locally. The QS3 slab still gives a fairly accurate prediction of the resultant force.

When subjected to blast loads, the shell element slab presents smaller maximum deflections than the solid element slab. After reaching maximum deflection, the shell slab deflection-time curves show a faster reflection back towards the zero position than the solid slab model. Hence the shell slab results can be said to be closer to the experimental results shown by Johansson (1978). However, the response is still not close to the experimental results and further studies should be made. As already stated by Bernhardsson & Forsén (2013) `*LOAD_BLAST_ENHANCED` underestimates the negative phase and a more accurate way of applying the blast load should be investigated.

Results from quasi static and blast load simulations emphasize the importance of using accurate material models. Overriding the default steel yield curve with a more accurate one is shown to be vital to get a functioning model at all. How the concrete characteristics affect the response is not investigated and should be studied further. The differences in results using a finer or courser mesh in the slab blast load simulations are here shown to be small. The gain in computational costs would in this particular case be greater than the loss in results. However, the slab structure is very simple and no definitive conclusions can be drawn.

As expected with regard to results from the slabs, simulated response of the building wall is generally more extensive than the experimental. Maximum upward force is however considerably lower in the simulations. When a load bearing building wall is bent an upward force will affect the overlying mass. Because of the use of thin shell elements, this force is likely not present. The maximum backward force for the simulation with reduced charge weight (F3) is bigger than for the full charge weight (F2). This is an inconsistency and should be investigated further.

The response of the blast loaded slabs is deflecting and reflecting whereas the external wall has more or less no reflecting response. The external wall structure is subjected to its own structural mass and simulated mass from the overlying stories. The slabs are not subjected

to any forces except from the blast load, making them able to reflect without resistance. Additionally, the underestimation of the negative phase in *LOAD_LAST_ENHANCED results in no or very small negative pressure pulling the structure back. Using different BLAST-modes with the LBE, i.e. *hemispherical surface burst* (1) and *spherical air burst* (2), is shown to have a big impact on the applied peak pressure on the building wall. The impact of using BLAST = 4, *air burst with ground reflection,* should be investigated as well.

When subjected to full charge weights, the ratio between simulated and experimental maximum deformation is shown to be higher for the external wall than for the slabs. When subjecting the slabs to reduced charge weights, generating a more true total impulse, the maximum deflections are smaller than the experimental results show. When subjecting the building wall to reduced charge weight and a more true total impulse, the maximum deflections are close to the experimental results. This indicates that the negative phase cannot be ignored and that the method of using reduced charge weights can compensate for the underestimation in LBE. For a structure which reaches maximum deformation before being subjected to the whole blast wave (i.e. only the positive phase), the negative phase is likely of minor importance. But if the maximum deformation is reached after being subjected to the whole blast wave (i.e. positive and negative phase), the negative phase is more likely important. Further investigations should be made before coming to any conclusions.

4.1. Conclusions

This thesis shows that reinforced concrete slab models based on shell element formulation can simulate the maximum deflection from a blast load with the same accuracy as models based on solid element formulation with smeared reinforcement.

The LS-DYNA *MAT_172 material model and the *PART_COMPOSITE element formulation function presents a simple method of constructing reinforced concrete slab models. *MAT_172 should be used with a more accurate steel stress-strain curve than the default ideal plastic.

The introduced shell element formulated slab model can be used to construct bigger concrete structure models for blast load response simulations. Further studies on simpler building components such as slabs should however be made beforehand. A first step is to investigate a more accurate way of applying the blast load including the negative phase.

5. References

WRITTEN

Barmejo, M., Goicolea, J.M., Gabaldón, F.S.A., 2011. *Impact and explosive loads on concrete buildings using shell and beam type elements*. 3:rd ECCOMAS Thematic conference on computational methods in structural dynamics and earthquake engineering, Corfu, Greece.

Bernhardsson, S., Forsén R., 2013. *Vapenverkan mot byggda konstruktioner*. FOI-D—0510—SE, Totalförsvarets forskningsinstitut, Grindsjön, Sweden.

Edin, K., Forsén R., 1991. *Vapenverkan mot flervånings betongbyggnad II – Bestämning av skador från 2,1 kg sfäriska hexotolladdningar mot husfasad i skala 1:4*. FOA rapport C20859-2.3, Försvarets forskningsanstalt, Sundbyberg, Sweden.

EN 1992-1-2:1995. *Eurocode 2: Design of concrete structures – Part 1-2: General rules – Structural fire design.* European Committee for standardization, Brussels, Belgium.

EN 1992-1-2:2004. *Eurocode 2: Design of concrete structures – Part 1-2: General rules – Structural fire design.* European Committee for standardization, Brussels, Belgium.

FOI, 2009. *Explosivämneskunskap: Kurskompendium 2011*. Totalförsvarets forskningsinstitut, Tumba, Sweden.

Hallquist, J., 2006. *LS-DYNA Theory Manual*. Livermore Software Technology Cooperation, Livermore, USA.

Isaksson, T., Mårtensson, A., 2010. *Byggkonstruktion: Regel- och formelsamling.* Studentlitteratur AB, Lund, Sweden.

Johansson, I., 1978. *Försök med enkelspända betongplattor utsatta för luftstötvågsbelastning*. FOA rapport C 20256-D4(A3), Stockholm, Sweden.

Johansson, M., 2002. *Stötvågsutbredning i luft*. Räddningsverket, Karlstad, Sweden.

Krauthammer, T., 2008. *Modern Protective Structures*. Taylor & Francis Group, Boca Raton, USA.

LSTC, 2013a. *LS-DYNA Keyword User's Manual: Volume 1*. Worcester, USA.

LSTC, 2013b. *LS-DYNA Keyword User's Manual: Volume 2–Material Models*. Worcester, USA.

Luccioni, B., Ambrosini, R., Danesi, R., 2004. *Analysis of building collapse under blast loads.* Engineering Structures no. 26, p.63-71.

Ottosen, N., Petersson, H., 1992. *Introduction to the Finite Element Method*. Prentice Hall Europe, Harlow, UK.

Phuvoravan, K., Sotelino, E., 2005. *Nonlinear finite element for reinforced concrete slabs*. Journal of Structural Engineering vol. 131 no. 4.

WEB SOURCES:

LSTC, 2013c. Livermore Software Technology Cooperation: http://www.lstc.com/products/ls-dyna (2013-08-20).

COMPUTER SOFTWARE:

Hyde, D.W., 1992. *ConWep – Conventional Weapons Effects.* U.S. Army Engineer Waterways Experiment Station, Vicksburg, USA.

Appendix A. Plate Theory

The theory of plates, or *shells*, is an engineering approximation where the original three-dimensional problem is described as a simpler two-dimensional problem (Ottosen & Petersson, 1992). The plate theory does not fulfill all the field equations, but for many engineering applications it provides realistic solutions. The first convincing plate theory was presented by Kirchhoff in 1850 (Ottosen & Petersson, 1992), however many other refined theories has been formulated since then.

A.1. Kirchhoff plate theory

Introducing a coordinate system, a plate is a structure symmetrically stretched out in the xy-plane, with a thickness *t* that is small compared to the other dimensions of the plate (Ottosen & Petersson, 1992). The plate is loaded by a transverse loading *q* measured positive in the z-direction as well as the deflection *w*. The plate configuration can be seen in Figure A.1.

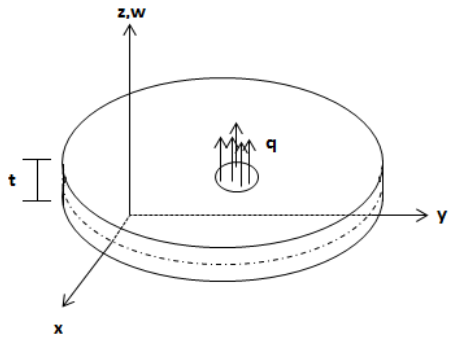

Figure A.1. Plate with loading q. Based on Ottosen & Petersson (1992).

A.1.1. Equilibrium conditions

The stress components σ_{xx}, σ_{xy}, σ_{xz} and $\sigma_{yx}, \sigma_{yy}, \sigma_{yz}$ exist for sections normal to the x- and y-axes and give rise to the following forces and moments:

$$V_{xz} = \int_{-t/2}^{t/2} \sigma_{xz} dz \tag{A.1}$$

$$V_{yz} = \int_{-t/2}^{t/2} \sigma_{yz} dz$$

$$M_{xx} = \int_{-t/2}^{t/2} z\sigma_{xx} dz$$

$$M_{yy} = \int_{-t/2}^{t/2} z\sigma_{yy} dz \tag{A.2}$$

$$M_{xy} = \int_{-t/2}^{t/2} z\sigma_{xy} dz$$

$$N_{xx} = \int_{-t/2}^{t/2} \sigma_{xx} dz$$

$$N_{yy} = \int_{-t/2}^{t/2} \sigma_{yy} dz \tag{A.3}$$

$$N_{xy} = N_{yx} = \int_{-t/2}^{t/2} \sigma_{xy} dz$$

The plate is assumed to have transverse force loading only, i.e. no resulting forces in the xy-plane. This makes horizontal equilibrium require that

$$N_{xx} = N_{yy} = N_{xy} = 0 \tag{A.4}$$

Considering an infinitesimally small part of the plate, all the forces acting on the part is shown in Figure 2.2.

Vertical equilibrium requires that

$$q dx dy - V_{yz} dx + \left(V_{xz} + \frac{\partial V_{xz}}{\partial x} dx\right) dy + \left(V_{yz} + \frac{\partial V_{yz}}{\partial y} dy\right) dx - V_{xy} dy = 0$$

$$\Rightarrow \frac{\partial V_{xz}}{\partial x} + \frac{\partial V_{yz}}{\partial y} + q = 0 \tag{A.5}$$

Moment equilibrium about the right side of the part, parallel to the x-axis, require that

$$qdxdy\frac{1}{2}dy + V_{yz}dxdy - \left(V_{xz} + \frac{\partial V_{xz}}{\partial x}dx\right)dy\frac{1}{2}dy + V_{xz}dy\frac{1}{2}dy$$

$$+M_{yy}dx - \left(M_{xy} + \frac{\partial M_{xy}}{\partial x}dx\right)dy - \left(M_{yy} + \frac{\partial M_{yy}}{\partial x}dy\right)dx + M_{xy}dy = 0$$

$$\Rightarrow q\frac{1}{2}dy + V_{yz} - \frac{\partial V_{xz}}{\partial x}\frac{1}{2}dy - \frac{\partial M_{xy}}{\partial x} - \frac{\partial M_{yy}}{\partial y} = 0 \qquad \text{(A.6)}$$

As dy is infinitely small

$$\frac{\partial M_{xy}}{\partial x} + \frac{\partial M_{yy}}{\partial y} = V_{yz} \qquad \text{(A.7)}$$

Moment equilibrium about one of the sides parallel to the y-axis in Figure A.2 is derived in a similar manner to

$$\frac{\partial M_{xx}}{\partial x} + \frac{\partial M_{xy}}{\partial y} = V_{xz} \qquad \text{(A.8)}$$

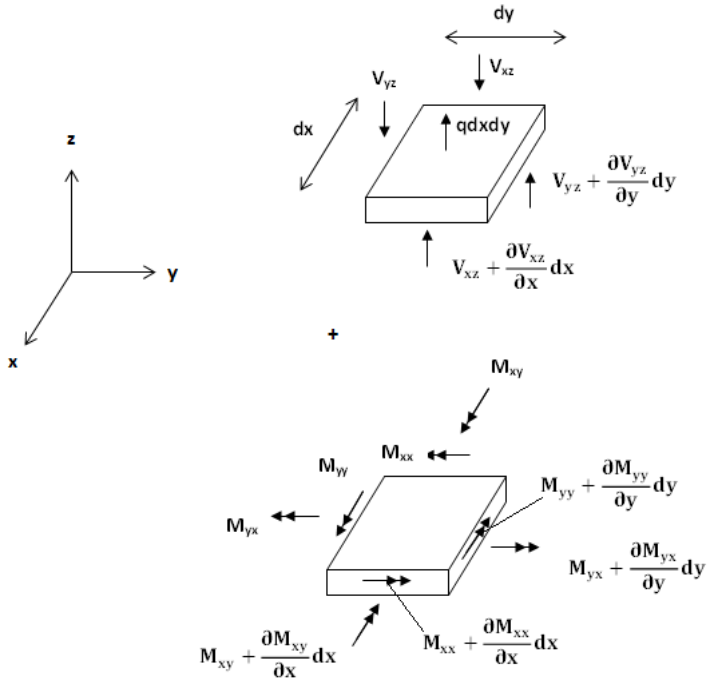

Figure A.2. Vertical shear forces and moments acting on an infinitesimally small part of the plate. Based on Ottosen & Petersson (1992).

A.1.2. Kinematic relations

Assuming that the plate deforms in accordance with Bernoulli's assumption for beam behavior (plane sections normal to the mid-plane remain plane and normal to the mid-plane during deformation), the x-, y- and z-displacements are defined as:

$$u_x = u^0 - z\frac{\partial w}{\partial x}$$
$$u_y = v^0 - z\frac{\partial w}{\partial y} \quad \text{(A.9)}$$
$$u_z = w$$

where $u^0$and v^0 are the displacements of the mid-plane in the x- and y-directions and

$u^0 = u^0(x,y);\ v^0 = v^0(x,y)$ and $w = w(x,y)$,

assuming that the deflection w is independent of z.

Strains given as

$$\varepsilon_{xx} = \frac{\partial u_x}{\partial x};\ \varepsilon_{yy} = \frac{\partial u_y}{\partial y};\ \ \varepsilon_{zz} = \frac{\partial u_z}{\partial z} \quad \text{(A.10)}$$

and

$$\gamma_{xy} = \frac{\partial u_x}{\partial y} + \frac{\partial u_y}{\partial x}$$
$$\gamma_{xz} = \frac{\partial u_x}{\partial z} + \frac{\partial u_z}{\partial x} \quad \text{(A.11)}$$
$$\gamma_{yz} = \frac{\partial u_y}{\partial z} + \frac{\partial u_z}{\partial y}$$

become

$$\varepsilon_{xx} = \frac{\partial u^0}{\partial x} - z\frac{\partial^2 w}{\partial x^2}$$
$$\varepsilon_{yy} = \frac{\partial v^0}{\partial y} - z\frac{\partial^2 w}{\partial y^2} \quad \text{(A.12)}$$
$$\gamma_{xy} = \frac{\partial u^0}{\partial y} + \frac{\partial v^0}{\partial x} - 2z\frac{\partial^2 w}{\partial x \partial y}$$

and

$$\varepsilon_{zz} = \gamma_{xz} = \gamma_{yz} = 0 \quad \text{(A.13)}$$

A.1.3. Constitutive relation

It is not possible to obtain a correspondence between the non-zero shear stresses σ_{xz} and σ_{yz} necessary to maintain equilibrium and the zero shear strains γ_{xz} and γ_{yz} (Ottosen & Petersson, 1992). Assuming that the plate is thin, the largest stresses will be $\sigma_{xx,}\sigma_{yy}$ and σ_{xy}. Together with the assumption that Hooke's law is applicable, it implies that

$$\boldsymbol{\sigma} = \boldsymbol{D\varepsilon} \tag{A.14}$$

where

$$\boldsymbol{\sigma} = \begin{bmatrix} \sigma_{xx} \\ \sigma_{yy} \\ \sigma_{zz} \end{bmatrix}; \quad \boldsymbol{\varepsilon} = \begin{bmatrix} \varepsilon_{xx} \\ \varepsilon_{yy} \\ \gamma_{xy} \end{bmatrix} \tag{A.15}$$

For isotropic elasticity, the plane stress constitutive matrix **D** is given by

$$\boldsymbol{D} = \frac{E}{1-v^2}\begin{bmatrix} 1 & v & 0 \\ v & 1 & 0 \\ 0 & 0 & \frac{1}{2}(1-v) \end{bmatrix} \tag{A.16}$$

With

$$\boldsymbol{\varepsilon^0} = \begin{bmatrix} \frac{\partial u^0}{\partial x} \\ \frac{\partial v^0}{\partial y} \\ \frac{\partial u^0}{\partial y} + \frac{\partial v^0}{\partial x} \end{bmatrix} \quad \text{and} \quad \boldsymbol{\kappa} = \begin{bmatrix} \frac{\partial^2 w}{\partial x^2} \\ \frac{\partial^2 w}{\partial y^2} \\ 2z\frac{\partial^2 w}{\partial x \partial y} \end{bmatrix} \tag{A.17}$$

where $\boldsymbol{\kappa}$ is called the curvature matrix (Ottosen & Petersson, 1992), the strains as given in (A.12) can be written as

$$\boldsymbol{\varepsilon} = \boldsymbol{\varepsilon^0} - z\boldsymbol{\kappa} \tag{A.18}$$

Together with (A.14) this yields

$$\boldsymbol{\sigma} = \boldsymbol{D\varepsilon^0} - z\boldsymbol{D\kappa} \tag{A.19}$$

Introducing the matrix

$$\boldsymbol{M} = \begin{bmatrix} M_{xx} \\ M_{yy} \\ M_{xy} \end{bmatrix} \tag{A.20}$$

the moments in (A.2) can be written as

$$\boldsymbol{M} = \int_{-t/2}^{t/2} z\boldsymbol{\sigma} dz \tag{A.21}$$

Assuming

$$\boldsymbol{D} = \boldsymbol{D}(x, y) \tag{A.22}$$

i.e. independent of z, and keeping in mind that $\boldsymbol{\varepsilon^0}$ and $\boldsymbol{\kappa}$ are independent of z, inserting (A.19) in (A.21) gives

$$\boldsymbol{M} = \boldsymbol{D\varepsilon^0} \int_{-t/2}^{t/2} z dz - \boldsymbol{D\kappa} \int_{-t/2}^{t/2} z^2 dz \tag{A.23}$$

The integrals

$$\int_{-t/2}^{t/2} z dz = 0$$

and

$$\int_{-t/2}^{t/2} z^2 dz = \frac{t^3}{12}\boldsymbol{D}$$

This means that, irrespective of the value of the strains, $\boldsymbol{\varepsilon^0}$, (A.23) can be reduced to

$$\boldsymbol{M} = -\widetilde{\boldsymbol{D}}\boldsymbol{\kappa}\,; \quad \widetilde{\boldsymbol{D}} = \frac{t^3}{12}\boldsymbol{D} \tag{A.24}$$

With $\boldsymbol{\sigma}$ defined as in (A.15), horizontal forces as given in (A.3) and using (A.19) yields

$$\begin{bmatrix} N_{xx} \\ N_{yy} \\ N_{xy} \end{bmatrix} = \boldsymbol{D\varepsilon^0} t \tag{A.25}$$

Without resulting forces acting in the mid-plane as stated in (A.4), it is concluded that

$$\boldsymbol{\varepsilon^0} = 0 \tag{A.26}$$

This shows that there is no straining in the mid-plane. If the horizontal forces would be different from zero, these are determined by the in-plane strains whereas moments are controlled by the curvature matrix, as given in (A.24) and (A.25) respectively. This implies that bending and straining of the mid-plane are uncoupled phenomena and can be treated separately if (A.22) is valid (Ottosen & Petersson, 1992).

A.1.4. Differential equations for plate theory

With (A.26) valid, (A.18) and (A.19) are reduced to

$$\boldsymbol{\varepsilon} = -z\boldsymbol{\kappa} \quad \text{and} \quad \boldsymbol{\sigma} = -z\boldsymbol{D}\boldsymbol{\kappa} \tag{A.27}$$

In the equilibrium conditions given by (A.5), (A.7) and (A.8), it is only the moments that can be expressed as kinematic quantities. By differentiating (A.8) and (A.7) with respect to x and y respectively and using (A.5), the shear forces V_{yz} and V_{xz} can be eliminated yielding

$$\frac{\partial^2 M_{xx}}{\partial x^2} + 2\frac{\partial^2 M_{xy}}{\partial x \partial y} + \frac{\partial^2 M_{yy}}{\partial y^2} + q = 0 \tag{A.28}$$

which holds irrespective of the constitutive assumption.

Introducing the matrix differential operator

$$\boldsymbol{\nabla} = \begin{bmatrix} \frac{\partial^2}{\partial x^2} \\ \frac{\partial^2}{\partial y^2} \\ 2\frac{\partial^2}{\partial x \partial y} \end{bmatrix} \tag{A.29}$$

(A.28) can be written as

$$\boldsymbol{\nabla}^T \boldsymbol{M} + q = 0 \tag{A.30}$$

and (A.17) can be written as

$$\boldsymbol{\kappa} = \boldsymbol{\nabla}\mathrm{w} \tag{A.31}$$

which put into (A.24) gives

$$\boldsymbol{M} = -\widetilde{\boldsymbol{D}}\boldsymbol{\nabla}\mathrm{w} \tag{A.32}$$

Using (A.32) in (A.30) yields the plate theory differential equation

$$\boldsymbol{\nabla}^T \widetilde{\boldsymbol{D}} \boldsymbol{\nabla}\mathrm{w} = q \tag{A.33}$$

When deflection w has been determined from (A.33), assuming that the thickness t is constant and that **D** is given by (A.16) and is independent of x and y, (A.33) becomes

$$\frac{\partial^4 w}{\partial x^4} + 2\frac{\partial^4 w}{\partial x^2 \partial y^2} + \frac{\partial^4 w}{\partial y^4} = \frac{12(1-\nu^2)}{Et^3} \tag{A.34}$$

A.2. Shell element formulation in LS-DYNA

LS-DYNA presents a variety of available shell element formulations. The default shell element formulation is the Belytchko-Lin-Tsay shell element, a computationally efficient alternative to the Hughes-Liu shell element first implemented in LS-DYNA (Hallquist, 2006).

The Hughes-Liu shell element was selected for LS-DYNA due to several qualities. Among them mentioned are:

- rigid body rotations do not generate strains;
- it is simple, giving computational efficiency and robustness;
- it is compatible with brick elements;
- it includes finite transverse shear strains.

The Hughes-Liu shell element is a degeneration of the standard 8-node brick element formulation. The isoperimetric mapping of an 8-node bi-unit cube is given as

$$x(\xi,\eta,\zeta) = N_a(\xi,\eta,\zeta)x_a \tag{A.35}$$

$$N_a(\xi,\eta,\zeta) = \frac{(1+\xi_a\xi)(1+\eta_a\eta)(1+\zeta_a\zeta)}{8} \tag{A.36}$$

where x is an arbitrary point in the element, (ξ,η,ζ) are the parametric coordinates, x_a are the global nodal coordinates of node a, and N_a are the element shape functions evaluated at node a. To create the shell element, the through thickness nodal pairs of the cube are combined into a single node, thus yielding the 4-node shell geometry. Thickness is defined of planes with constant ζ, usually only defined at the nodes and referred to as 'nodal fibers' (Hallquist, 2006). The mapping of the bi-unit cube into the shell element (shown in Figure A.3) is separated into two parts;

$$x(\xi,\eta,\zeta) = \bar{x}(\xi,\eta) + X(\xi,\eta,\zeta) \tag{A.37}$$

where $\bar{x}$ is a position vector to a point on the reference surface of the shell and X is a position vector, based at point $\bar{x}$ on the reference surface, defining the fiber direction through that point. Considering one of the points defining the reference surface

$$\bar{x}(\xi,\eta) = N_a(\xi,\eta)\bar{x}_a \tag{A.38}$$

$$X(\xi,\eta,\zeta) = N_a(\xi,\eta)X_a(\zeta) \tag{A.39}$$

Arbitrary points in the reference surface $\bar{x}$ are interpolated by the shape function $N(\xi,\eta)$, whereas points of the reference surface are further interpolated by using a shape function along the fiber direction, $X(\zeta)$, where

$$X_a(\zeta) = z_a(\zeta)\hat{X}_a \tag{A.40}$$

$$z_a = N_+(\zeta)z_a^+ + N_-(\zeta)z_a^- \quad \text{(A.41)}$$

$$N_+(\zeta) = \frac{1+\zeta}{2} \quad \text{(A.42)}$$

$$N_-(\zeta) = \frac{1-\zeta}{2} \quad \text{(A.43)}$$

and $\hat{X}_a$ is a unit vector in the fiber direction and $z(\zeta)$ is a thickness function, as shown in Figure A.3.

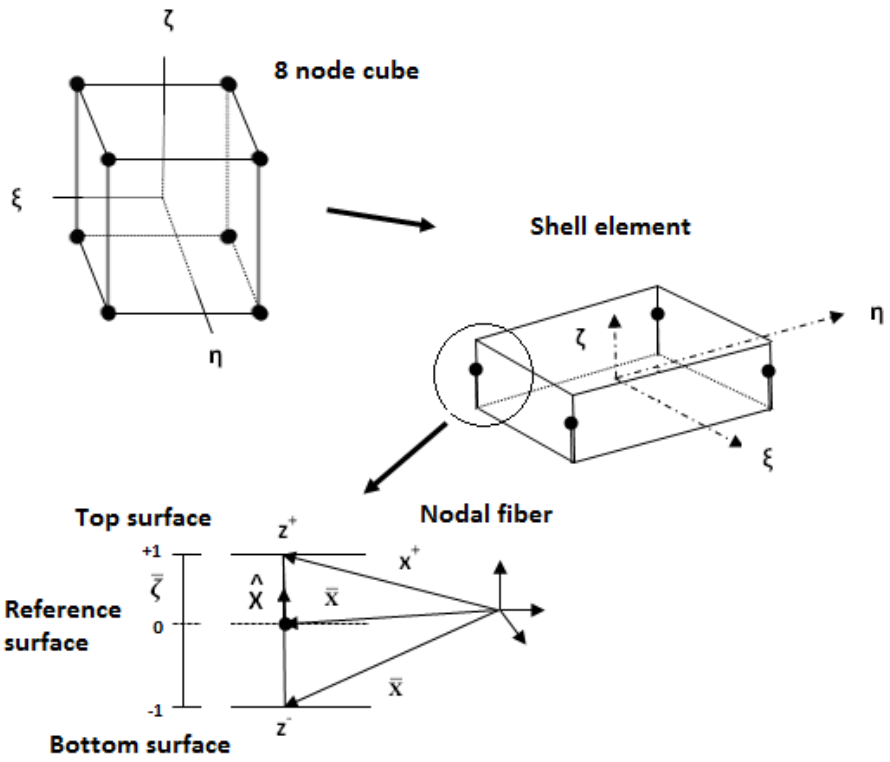

Figur A.3. Mapping of the bi-unit cube into the Hughes-Liu shell element showing the nodal fiber nomenclature. Based on Hallquist (2006).

Appendix B. Soil, rock and concrete models in LS-DYNA

Compilation by Sebastian Bernhardsson, FOI.

Soil, Concrete and Rock Models (971 R6.0.0)

	Features included in the model									Element formulations supported by the model					
Model	STRATE	FAIL	EOS	THERM	ANISO	DAM	TENS	AUTO	REINF	SOLID	LH-BEAM	D-BEAM	SHELL	T-SHELL	SPH	MMALE
5 Soil and Foam							x			x				x	x	x
14 Soil and Foam with Failure		x					x			x				x	x	x
16 Pseudo Tensor Geological Model	x	x	x			x	x	x	x	x				x	x	x
25 Inviscid Two Invariant Geological Cap		x					x			x				x	x	
26 Honeycomb	x	x			x		x			x				x		
72 Concrete Damage	x	x	x			x	x		x	x				x	x	x
72R3 Concrete Damage	x	x	x			x	x	x		x				x	x	
78 Soil Concrete		x				x	x			x				x		x
79 Hysteretic Soil (Elasto-Perfectly Plastic)		x					x			x				x	x	x
80 Ramberg-Osgood										x				x		x
84 Winfrith Concrete (w/ rate effects)	x						x		x	x						x
85 Winfrith Concrete							x		x	x						x
96 Brittle Damage	x	x			x	x	x		x	x						x
111 Johnson-Holmquist Concrete	x	x				x	x			x				x	x	
126 Modified Honeycomb	x	x			x	x	x			x				x		
145 Schwer-Murray Cap Model	x	x				x	x			x					x	
146 1DOF Generalized Spring	x											x				
147 FWHA Soil	x					x	x			x				x	x	x
147N FHWA Soil Nebraska	x					x	x	x		x				x	x	x
159 CSCM	x	x				x	x	x		x				x	x	
172 Concrete EC2	x			x			x	x	x		x		x	x		
173 Mohr Coulomb					x		x			x					x	
174 RC Beam						x	x		x		x					
192 Soil Brick										x				x		
193 Drucker Prager							x			x				x		
198 Jointed Rock		x			x		x			x						
230 Elastic Perfectly Matched Layer (PML)	x									x						
232 Biot Linear Hysteretic Material	x									x			x	x		
237 Biot Hysteretic PML	x									x						
245 Orthotropic/anisotropic PML	x									x						
272 RHT concrete model	x	x				x	x	x		x						

Key to Soil, concrete and rock models:

STRATE - Strain-rate effects
FAIL – Failure criteria
EOS - EOS required for 3D solids and 2D continuum elements
THERM - Thermal effects
ANISO - Anisotropic/orthotropic
DAM – Damage effects
TENS - Tension handled differently than compression
AUTO - Automatic internal generation of a simple "generic" concrete model
REINF - Mixed model with fraction of reinforcement

SOLID – Solid elements
LH-BEAM - Hughes-Liu beam
D-BEAM - Discrete beam
SHELL - Shells
T-SHELL - Thick shell formulation 1, 2, 3, or 5 (Note! Check which formulation is valid, usually 3 & 5)
SPH - SPH element
MMALE - Multi-material ALE solid (Note! Not always validated)

Appendix C. QS2 LS-DYNA ASCII code

```
$# LS-DYNA Keyword file created by LS-PrePost 4.0 - 24Aug2013(02:00)
$# Created on Sep-30-2013 (10:07:00)
*KEYWORD
*TITLE
$# title
LS-DYNA keyword deck by LS-PrePost
$
$$$$ UNITS: mm, ms, kg, kN, GPa
$
$$$$ PARTS & SECTION
$
$
*PART
$# title
Support
$#     pid     secid       mid     eosid      hgid      grav    adpopt      tmid
         1         3         4         0         0         0         0         0
*SECTION_SHELL_TITLE
Support shell
$#   secid    elform      shrf       nip     propt   qr/irid     icomp     setyp
         3         1  1.000000         4         1         0         0         1
$#      t1        t2        t3        t4      nloc     marea      idof    edgset
  1.000000  1.000000  1.000000  1.000000     0.000     0.000     0.000         0
*PART_COMPOSITE
$# title
Slab
$#     pid    elform      shrf      nloc     marea      hgid    adpopt  ithelfrm
         2         2  0.000000     0.000     0.000         1         0         0
$#    mid1    thick1        b1    ithid1      mid2    thick2        b2    ithid2
         1 12.750000     0.000         0         1 12.750000     0.000         0
         1 12.750000     0.000         0         1 12.750000     0.000         0
         1 12.750000     0.000         0         1 12.750000     0.000         0
         1 12.750000     0.000         0         1 12.750000     0.000         0
         1 12.750000     0.000         0         1 12.750000     0.000         0
         2 12.750000     0.000         0         1 12.750000     0.000         0
$
$
$$$$ MATERIALS
$
$
*MAT_CONCRETE_EC2_TITLE
Concrete
$#     mid        ro        fc        ft     typec     unitc    ecuten      fcc6
         1 2.3400E-6  0.030000  0.003800  1.000000 1000.0000     0.000     0.000
$# esoft       lchar        mu    taumxf    taumxc    ecragg     aggsz     unitl
              0.000     0.000     0.000     0.000     0.000     0.000     0.000
$# ymreinf    prrinf   sureinf     typer    fracrx    fracry     lcrsu    lcalps
 200.00000  0.300000  0.500000  1.000000     0.000     0.000         0         0
$#    aopt      et36    prt36     ecut36    lcalpc    degrad    ishchk    unlfac
     0.000 33.000000  0.2500001.0000E+20         0     0.000         0  0.500000
*MAT_CONCRETE_EC2_TITLE
Reinforcement
$#     mid        ro        fc        ft     typec     unitc    ecuten      fcc6
         2 2.3400E-6  0.030000  0.003800  1.000000 1000.0000     0.000     0.000
$# esoft       lchar        mu    taumxf    taumxc    ecragg     aggsz     unitl
              0.000     0.000     0.000     0.000     0.000     0.000     0.000
$# ymreinf    prrinf   sureinf     typer    fracrx    fracry     lcrsu    lcalps
 200.00000  0.300000  0.500000  5.000000  0.002000  0.010000         3         0
$#    aopt      et36    prt36     ecut36    lcalpc    degrad    ishchk    unlfac
     0.000 33.000000  0.2500001.0000E+20         0     0.000         0  0.500000
```

```
*MAT_RIGID_TITLE
Support
$#     mid        ro         e        pr         n    couple         m     alias
         4 1.0000E-5 200.00000  0.300000     0.000     0.000     0.000
$#     cmo      con1      con2
     0.000         0         0
$# lco or a1      a2        a3        v1        v2        v3
     0.000     0.000     0.000     0.000     0.000     0.000
$
$
$$$$ SLAB-SUPPORT CONTACT & BOUNDARIES
$
$
*CONTACT_AUTOMATIC_NODES_TO_SURFACE_ID
$#     cid                                                              title
         1
$#    ssid      msid     sstyp     mstyp    sboxid    mboxid       spr       mpr
         1         2         3         3         0         0         0         0
$#      fs        fd        dc        vc       vdc    penchk        bt        dt
     0.000     0.000     0.000     0.000 20.000000         0     0.0001.0000E+20
$#     sfs       sfm       sst       mst      sfst      sfmt       fsf       vsf
  1.000000  1.000000     0.000     0.000  1.000000  1.000000  1.000000  1.000000
$ LOAD
*BOUNDARY_PRESCRIBED_MOTION_SET
$#    nsid       dof       vad      lcid        sf       vid     death     birth
         1         3         2         1  1.000000         01.0000E+28     0.000
$ SUPPORT PRESCRIBED ZERO MOTION
*BOUNDARY_PRESCRIBED_MOTION_RIGID_ID
$#      id                                                           heading
         1
$#     pid       dof       vad      lcid        sf       vid     death     birth
         1         1         2         2  1.000000         01.0000E+28     0.000
$#     pid       dof       vad      lcid        sf       vid     death     birth
         1         2         2         2  1.000000         01.0000E+28     0.000
$#     pid       dof       vad      lcid        sf       vid     death     birth
         1         3         2         2  1.000000         01.0000E+28     0.000
$#     pid       dof       vad      lcid        sf       vid     death     birth
         1         5         2         2  1.000000         01.0000E+28     0.000
$#     pid       dof       vad      lcid        sf       vid     death     birth
         1         6         2         2  1.000000         01.0000E+28     0.000
$#     pid       dof       vad      lcid        sf       vid     death     birth
         1         7         2         2  1.000000         01.0000E+28     0.000
$ SLAB CORNER NODES LOCKED IN X
*BOUNDARY_SPC_SET
$#    nsid       cid      dofx      dofy      dofz     dofrx     dofry     dofrz
         2         0         1         0         0         0         0         0
*SET_NODE_LIST
$#     sid       da1       da2       da3       da4    solver
         2     0.000     0.000     0.000     0.000      MECH
$#    nid1      nid2      nid3      nid4      nid5      nid6      nid7      nid8
     13274     13300     10520     10546         0         0         0         0
$
$
$$$$ OUTPUT FUNCTIONS
$
$
$
*DATABASE_BNDOUT
$#      dt    binary      lcur     ioopt
 100.00000         0         0         1
*DATABASE_ELOUT
$#      dt    binary      lcur     ioopt   option1   option2   option3   option4
 100.00000         0         0         1         0         0         0         0
*DATABASE_GLSTAT
$#      dt    binary      lcur     ioopt
 100.00000         0         0         1
```

```
*DATABASE_MATSUM
$#      dt    binary      lcur     ioopt
 100.00000         0         0         1
*DATABASE_NODOUT
$#      dt    binary      lcur     ioopt   option1   option2
 100.00000         0         0         1     0.000         0
*DATABASE_BINARY_D3PLOT
$#      dt      lcdt      beam     npltc    psetid
 100.00000         0         0         0         0
$#   ioopt
         0
*DATABASE_HISTORY_NODE
$#     id1       id2       id3       id4       id5       id6       id7       id8
     11896     11734     11464     11194     10762         0         0         0
$
$
$$$$ CONTROL FUNCTIONS
$
$
$
*CONTROL_HOURGLASS
$#     ihq        qh
         1  0.100000
*CONTROL_TERMINATION
$#  endtim    endcyc     dtmin    endeng    endmas
 1000.0000         0     0.000     0.000     0.000
*CONTROL_TIMESTEP
$#  dtinit    tssfac      isdo    tslimt     dt2ms      lctm     erode     ms1st
     0.000  0.800000         0     0.000     0.000         0         0         0
$#  dt2msf   dt2mslc     imscl    unused    unused     rmscl
     0.000         0         0                       0.000
*HOURGLASS
$#    hgid       ihq        qm       ibq        q1        q2    qb/vdc        qw
         1         4  0.050000         0  1.500000  0.060000  0.100000  0.100000
$
$
$$$ CURVES DEFINING DEFLECTION, SUPPORT MOTION AND STEEL YIELD CURVE
$
$
*DEFINE_CURVE
$#    lcid      sidr       sfa       sfo      offa      offo    dattyp
         1         0  1.000000  1.000000     0.000     0.000         0
$#               a1                  o1
             0.000               0.000
         10001.000          -250.00000
*DEFINE_CURVE
$#    lcid      sidr       sfa       sfo      offa      offo    dattyp
         2         0  1.000000  1.000000     0.000     0.000         0
$#               a1                  o1
             0.000               0.000
         10001.000               0.000
*DEFINE_CURVE
$#    lcid      sidr       sfa       sfo      offa      offo    dattyp
         3         0  1.000000  1.000000     0.000     0.000         0
$#               a1                  o1
             0.000            1.000000
          0.220000            1.462000
          0.270000               0.000
$
$
$$$ INCLUDE FILES FOR NODE & ELEMENT DATA
$
$
*INCLUDE
Support.k
*INCLUDE
nodes.k
*END
```

Appendix D. *MAT_172 variable description

From LS-DYNA Keyword user's manual Volume II – Material Models (2013).

MID	Material identification. A unique number or label not exceeding 8 characters must be specified.
RO	Mass density
FC	Compressive strength of concrete (stress units)
FT	Tensile stress to cause cracking
TYPEC	Concrete aggregate type for stress-strain-temperature relationships EQ.1.0: Siliceous (default), relationships from Draft EC2 ANNEX EQ.2.0: Calcareous, relationships from Draft EC2 ANNEX EQ.3.0: Non-thermally-sensitive using ET3, ECU3 EQ.4.0: Lightweight EQ.5.0: Fibre-reinforced EQ.6.0: Non-thermally-sensitive, Mander algorithm EC.7.0: Siliceous, relationships from EC2 2004 EC 8.0 Calcareous, relationships from EC2 2004
UNITC	Factor to convert stress units to MPa (used in shear capacity checks) e.g. if model units are Newtons and metres, UNITC=1E-6
ECUTEN	Strain to fully open a crack.
FCC6	Compressive strength of confined concrete (type 6). If blank, unconfined properties are assumed.
ESOFT	Tension stiffening (Slope of stress-strain curve post-cracking in tension)
MU	Friction on crack planes (max shear = mu*compressive stress)
TAUMXF	Maximum friction shear stress on crack planes (ignored if AGGSZ>0 - see notes).
TAUMXC	Maximum through-thickness shear stress after cracking (see notes). ECRAGG Strain parameter for aggregate interlock (ignored if AGGSZ>0 - see notes).
AGGSZ	Aggregate size (length units - used in NS3473 aggregate interlock formula - see notes).
UNITL	Factor to convert length units to millimetres (used only if AGGSZ>0 - see notes) e.g. if model unit is metres, UNITL=1000.
LCHAR	Characteristic length at which ESOFT applies, also used as crack spacing in aggregate-interlock calculation
YMREINF	Young's Modulus of reinforcement
PRREINF	Poisson's Ratio of reinforcement
SUREINF	Ultimate stress of reinforcement
TYPER	Type of reinforcement for stress-strain-temperature relationships EQ.1.0: Hot rolled reinforcing steel, from Draft EC2 Annex EQ.2.0: Cold worked reinforcing steel (default), from Draft EC2 EQ.3.0: Quenched and tempered prestressing steel

	EQ.4.0: Cold worked prestressing steel EQ.5.0: Non-thermally sensitive using loadcurve LCRSU. EQ.7.0: Hot rolled reinforcing steel, from EC2 2004 EQ 8.0: Cold worked reinforcing steel, from EC2 2004
FRACRX	Fraction of reinforcement (x-axis) (e.g. for 1% reinforcement FRACR=0.01).
FRACRY	Fraction of reinforcement (y-axis) (e.g. for 1% reinforcement FRACR=0.01).
LCRSU	Loadcurve for TYPER=5, giving non-dimensional factor on SUREINF versus plastic strain (overrides stress-strain relationships from EC2).
LCALPS	Optional loadcurve giving thermal expansion coefficient of reinforcement vs temperature – overrides relationship from EC2.
AOPT	Option for local orthotropic axes – see Material Type 2 EQ.0.0: locally orthotropic with material axes determined by element nodes as shown in Figure 2-3. Nodes 1, 2, and 4 of an element are identical to the nodes used for the definition of a coordinate system as by *DEFINE_COORDINATE_NODES. When this option is used in two-dimensional planar and axisymmetric analysis, it is critical that the nodes in the element definition be numbered counterclockwise for this option to work correctly. EQ.1.0: locally orthotropic with material axes determined by a point in space and the global location of the element center; this is the adirection. This option is for solid elements only. EQ.2.0: globally orthotropic with material axes determined by vectors defined below, as with *DEFINE_COORDINATE_ VECTOR. EQ.3.0: locally orthotropic material axes determined by rotating the material axes about the element normal by an angle, BETA, from a line in the plane of the element defined by the cross product of the vector **v** with the element normal. The plane of a solid element is the midsurface between the inner surface and outer surface defined by the first four nodes and the last four nodes of the connectivity of the element, respectively. LT.0.0: This option has not yet been implemented for this material model.
ET36	Youngs Modulus of concrete (TYPEC=3 and 6).
PRT36	Poissons Ratio of concrete (TYPEC=3 and 6).
ECUT36	Strain to failure of concrete in compression □cu (TYPEC=3 and 6).
LCALPC	Optional loadcurve giving thermal expansion coefficient of concrete vs temperature – overrides relationship from EC2.
DEGRAD	If non-zero, the compressive strength of concrete parallel to an open crack will be reduced (see notes).
ISHCHK	Flag = 1 to input data for shear capacity check.
UNLFAC	Stiffness degradation factor after crushing (0.0 to 1.0 – see notes).
XP, YP, ZP	Coordinates of point p for AOPT = 1 and 4 (see Mat type 2).
A1, A2, A3	Components of vector a for AOPT = 2 (see Mat type 2).
V1, V2, V3	Components of vector v for AOPT = 3 and 4 (see Mat type 2).

D1, D2, D3	Components of vector d for AOPT = 2 (see Mat type 2).
TYPESC	Type of shear capacity check EQ.1.0: BS 8110 EQ.2.0:ACI
P_OR_F	If BS8110 shear check, percent reinforcement – e.g. if 0.5%, input 0.5. If ACI shear check, ratio (cylinder strength/FC) - defaults to 1.
EFFD	Effective section depth (length units), used in shear capacity check. This is usually the section depth excluding the cover concrete.
GAMSC	Load factor used in BS8110 shear capacity check.
EC1_6	Strain at maximum compressive stress for Type 6 concrete.
ECSP_6	Spalling strain in compression for Type 6 concrete.

Appendix E. LB1 LS-DYNA ASCII code

```
$# LS-DYNA Keyword file created by LS-PrePost 4.0 - 24Aug2013(02:00)
$# Created on Sep-27-2013 (15:46:32)
*KEYWORD
*TITLE
$# title
LS-DYNA keyword deck by LS-PrePost
$
$$$$ UNITS: mm, ms, kg, kN, GPa
$
$ LOAD BLAST ENHANCED (HERE P2b DATA)
$
$
*LOAD_BLAST_SEGMENT_SET
$#     bid      ssid    alepid     sfnrb    scalep
         1         1         0     0.000  1.000000
*LOAD_BLAST_ENHANCED
$#     bid         m       xbo       ybo       zbo       tbo      unit     blast
         1 48.200000     0.000 1320.0000 8953.0000     0.000         6         1
$#     cfm       cfl       cft       cfp     nidbo     death    negphs
     0.000     0.000  1.000000     0.000         01.0000E+20         0
$
$
$$$$ PARTS & SECTION
$
$
*PART
$# title
Support
$#     pid     secid       mid     eosid      hgid      grav    adpopt      tmid
         1         3         4         0         0         0         0         0
*SECTION_SHELL_TITLE
Support shell
$#   secid    elform      shrf       nip     propt   qr/irid     icomp     setyp
         3         1  1.000000         4         1         0         0         1
$#      t1        t2        t3        t4      nloc     marea      idof    edgset
  1.000000  1.000000  1.000000  1.000000     0.000     0.000     0.000         0
*PART_COMPOSITE
$# title
Slab
$#     pid    elform      shrf      nloc     marea      hgid    adpopt  ithelfrm
         2         2  1.000000     0.000     0.000         0         0         0
$#    mid1    thick1        b1    ithid1      mid2    thick2        b2    ithid2
         1 12.750000     0.000         0         1 12.750000     0.000         0
         1 12.750000     0.000         0         1 12.750000     0.000         0
         1 12.750000     0.000         0         1 12.750000     0.000         0
         1 12.750000     0.000         0         1 12.750000     0.000         0
         1 12.750000     0.000         0         1 12.750000     0.000         0
         2 12.750000     0.000         0         1 12.750000     0.000         0
$
$
$$$$ MATERIALS
$
$
*MAT_CONCRETE_EC2_TITLE
Conc
$#     mid        ro        fc        ft     typec     unitc    ecuten      fcc6
         1 2.3400E-6  0.030000  0.003800  1.000000 1000.0000  0.002500  0.030000
$# esoft       lchar        mu    taumxf    taumxc    ecragg     aggsz     unitl
             0.000  0.4000001.0000E+20  0.004400  0.001000     0.000  1.000000
$# ymreinf    prrinf   sureinf     typer    fracrx    fracry     lcrsu    lcalps
 200.00000  0.300000  0.500000  1.000000     0.000     0.000         0         0
$#    aopt      et36     prt36     ecut36    lcalpc    degrad    ishchk    unlfac
     0.000 33.000000  0.2500001.0000E+20         0     0.000         0  0.500000
```

```
*MAT_CONCRETE_EC2_TITLE
Reinf
$#     mid        ro        fc        ft     typec     unitc    ecuten      fcc6
         2 2.3400E-6  0.030000  0.003800  1.000000 1000.0000  0.002500  0.030000
$# esoft       lchar        mu    taumxf    taumxc    ecragg     aggsz     unitl
             0.000  0.4000001.0000E+20  0.004400  0.001000     0.000  1.000000
$# ymreinf    prrinf   sureinf     typer    fracrx    fracry     lcrsu    lcalps
 200.00000  0.300000  0.500000  5.000000  0.020000  0.010000         3         0
$#    aopt      et36    prt36     ecut36    lcalpc    degrad    ishchk    unlfac
     0.000 33.000000  0.2500001.0000E+20         0     0.000         0  0.500000

*MAT_RIGID_TITLE
Support
$#     mid        ro         e        pr         n    couple         m     alias
         4 1.0000E-5 200.00000  0.300000     0.000     0.000     0.000
$#     cmo      con1      con2
     0.000         0         0
$# lco or a1      a2        a3        v1        v2        v3
     0.000     0.000     0.000     0.000     0.000     0.000
$
$
$$$$ SLAB-SUPPORT CONTACT & BOUNDARIES
$
$
*CONTACT_AUTOMATIC_NODES_TO_SURFACE_ID
$#     cid                                                                title
         1
$#    ssid      msid     sstyp     mstyp    sboxid    mboxid       spr       mpr
         1         2         3         3         0         0         0         0
$#      fs        fd        dc        vc       vdc    penchk        bt        dt
     0.000     0.000     0.000     0.000 20.000000         0     0.0001.0000E+20
$#     sfs       sfm       sst       mst      sfst      sfmt       fsf       vsf
  1.000000  1.000000     0.000     0.000  1.000000  1.000000  1.000000  1.000000
*BOUNDARY_PRESCRIBED_MOTION_RIGID_ID
$#      id                                                               heading
         1
$#     pid       dof       vad      lcid        sf       vid     death     birth
         1         1         2         2  1.000000         01.0000E+28     0.000
$#     pid       dof       vad      lcid        sf       vid     death     birth
         1         2         2         2  1.000000         01.0000E+28     0.000
$#     pid       dof       vad      lcid        sf       vid     death     birth
         1         3         2         2  1.000000         01.0000E+28     0.000
$#     pid       dof       vad      lcid        sf       vid     death     birth
         1         5         2         2  1.000000         01.0000E+28     0.000
$#     pid       dof       vad      lcid        sf       vid     death     birth
         1         6         2         2  1.000000         01.0000E+28     0.000
$#     pid       dof       vad      lcid        sf       vid     death     birth
         1         7         2         2  1.000000         01.0000E+28     0.000
*BOUNDARY_SPC_SET
$#    nsid       cid      dofx      dofy      dofz     dofrx     dofry     dofrz
         2         0         1         0         0         0         0         0
$
$
$$$$ OUTPUT FUNCTIONS
$
$
$
*DATABASE_BNDOUT
$#      dt    binary      lcur     ioopt
  0.100000         0         0         1
*DATABASE_GLSTAT
$#      dt    binary      lcur     ioopt
  0.100000         0         0         1
*DATABASE_MATSUM
$#      dt    binary      lcur     ioopt
  0.100000         0         0         1
```

```
*DATABASE_NODOUT
$#      dt    binary      lcur     ioopt   option1   option2
  0.001000         0         0         1     0.000         0
*DATABASE_BINARY_D3PLOT
$#      dt      lcdt      beam     npltc    psetid
     0.000         0         0        20         0
$#   ioopt
         0
*DATABASE_HISTORY_NODE
$#     id1       id2       id3       id4       id5       id6       id7       id8
     11896     11734     11464     11194     10762         0         0         0
$
$
$$$$ CONTROL FUNCTIONS
$
$
$
*CONTROL_HOURGLASS
$#     ihq        qh
         1  0.100000
*CONTROL_TERMINATION
$#  endtim    endcyc     dtmin    endeng    endmas
 150.00000         0     0.000     0.000     0.000
*CONTROL_TIMESTEP
$#  dtinit    tssfac      isdo    tslimt     dt2ms      lctm     erode     ms1st
     0.000  0.670000         0     0.000     0.000         0         0         0
$#  dt2msf   dt2mslc     imscl    unused    unused     rmscl
     0.000         0         0                       0.000
$
$
$$$ CURVES DEFINING BOUNDARY MOTIONS AND STEEL YIELD CURVE
$
$
*DEFINE_CURVE
$#    lcid      sidr       sfa       sfo      offa      offo    dattyp
         2         0  1.000000  1.000000     0.000     0.000         0
$#                a1                  o1
             0.000               0.000
         10001.000               0.000
*DEFINE_CURVE
$#    lcid      sidr       sfa       sfo      offa      offo    dattyp
         3         0  1.000000  1.000000     0.000     0.000         0
$#                a1                  o1
             0.000            1.000000
          0.220000            1.462000
          0.270000               0.000
$
$
$$$ INCLUDE FILES FOR NODE & ELEMENT DATA
$
$
*INCLUDE
Support.k
*INCLUDE
nodes.k
*END
```

Appendix F. External wall reinforcement drawing

From Edin & Forsén (1991).

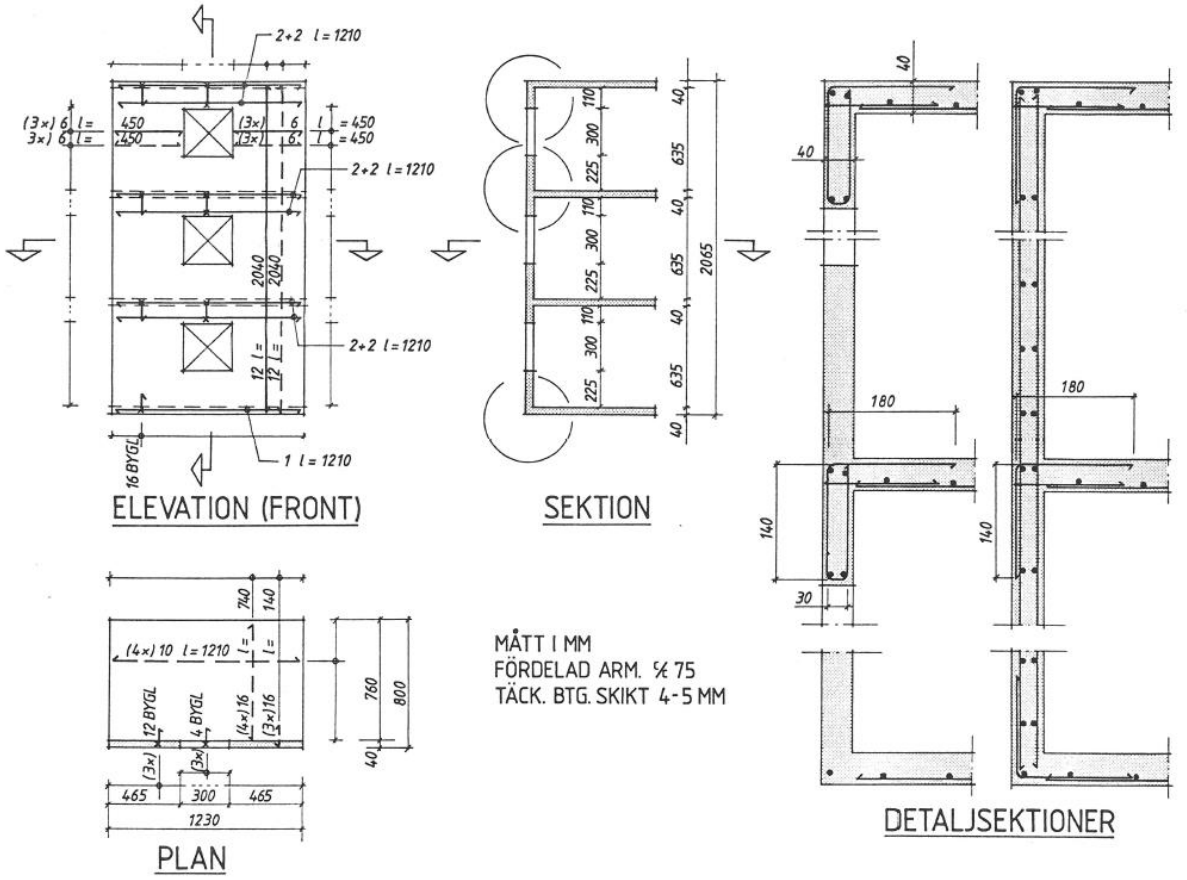

Appendix G. External building wall LS-DYNA ASCII code

```
$# LS-DYNA Keyword file created by LS-PrePost 4.0 - 07Jun2013(08:00)
$# Created on Oct-21-2013 (10:51:55)
*KEYWORD
$
$$$$ UNITS: mm, ms, kg, kN, GPa
$
$$$$ CONTROL FUNCTIONS
$
$
$
*CONTROL_TERMINATION
$#  endtim    endcyc     dtmin    endeng    endmas
 20.000000         0     0.000     0.000     0.000
*CONTROL_TIMESTEP
$#  dtinit    tssfac      isdo    tslimt     dt2ms      lctm     erode     ms1st
     0.000  0.670000         0     0.000     0.000         0         0         0
$#  dt2msf   dt2mslc     imscl    unused    unused     rmscl
     0.000         0         0                         0.000
$
$
$$$$ OUTPUT FUNCTIONS
$
$
$
$
*DATABASE_BNDOUT
$#      dt    binary      lcur     ioopt
  1.000000         0         0         1
*DATABASE_GLSTAT
$#      dt    binary      lcur     ioopt
  1.000000         0         0         1
*DATABASE_MATSUM
$#      dt    binary      lcur     ioopt
  1.000000         0         0         1
*DATABASE_NODOUT
$#      dt    binary      lcur     ioopt   option1   option2
  0.100000         0         0         1     0.000         0
*DATABASE_RCFORC
$#      dt    binary      lcur     ioopt
  1.000000         0         0         1
*DATABASE_BINARY_BLSTFOR
$#      dt      lcdt      beam     npltc    psetid
     0.000         1         0         0         0
*DATABASE_HISTORY_NODE
$#     id1       id2       id3       id4       id5       id6       id7       id8
      3078      4465      2809      2804         0         0         0         0
$
$
$
$
$$$$ SLAB-WALL CONTACTS & BOUNDARIES
$
$
$
*CONTACT_TIED_SHELL_EDGE_TO_SURFACE_OFFSET
$#     cid                                                               title
$#    ssid      msid     sstyp     mstyp    sboxid    mboxid       spr       mpr
         2         1         3         3         0         0         0         0
$#      fs        fd        dc        vc       vdc    penchk        bt        dt
     0.000     0.000     0.000     0.000     0.000         0     0.0001.0000E+20
$#     sfs       sfm       sst       mst      sfst      sfmt       fsf       vsf
  1.000000  1.000000     0.000 20.000000  1.000000  1.000000  1.000000  1.000000
```

```
*CONTACT_TIED_SHELL_EDGE_TO_SURFACE_OFFSET_ID
$#     cid                                                                  title
         2
$#    ssid      msid     sstyp     mstyp    sboxid    mboxid       spr       mpr
         3         1         3         3         0         0         0         0
$#      fs        fd        dc        vc       vdc    penchk        bt        dt
     0.000     0.000     0.000     0.000     0.000         0     0.0001.0000E+20
$#     sfs       sfm       sst       mst      sfst      sfmt       fsf       vsf
  1.000000  1.000000     0.000 20.000000  1.000000  1.000000  1.000000  1.000000
*CONTACT_TIED_SHELL_EDGE_TO_SURFACE_OFFSET_ID
$#     cid                                                                  title
         3
$#    ssid      msid     sstyp     mstyp    sboxid    mboxid       spr       mpr
         4         1         3         3         0         0         0         0
$#      fs        fd        dc        vc       vdc    penchk        bt        dt
     0.000     0.000     0.000     0.000     0.000         0     0.0001.0000E+20
$#     sfs       sfm       sst       mst      sfst      sfmt       fsf       vsf
  1.000000  1.000000     0.000 20.000000  1.000000  1.000000  1.000000  1.000000
*CONTACT_TIED_SHELL_EDGE_TO_SURFACE_OFFSET_ID
$#     cid                                                                  title
         4
$#    ssid      msid     sstyp     mstyp    sboxid    mboxid       spr       mpr
         5         1         3         3         0         0         0         0
$#      fs        fd        dc        vc       vdc    penchk        bt        dt
     0.000     0.000     0.000     0.000     0.000         0     0.0001.0000E+20
$#     sfs       sfm       sst       mst      sfst      sfmt       fsf       vsf
  1.000000  1.000000     0.000 20.000000  1.000000  1.000000  1.000000  1.000000
*BOUNDARY_PRESCRIBED_MOTION_SET_ID
$#      id                                                               heading
         1Floor 3 X
$#    nsid       dof       vad      lcid        sf       vid     death     birth
         3         1         2         2  1.000000         01.0000E+28     0.000
$#      id                                                               heading
         2Floor 3 Y
$#    nsid       dof       vad      lcid        sf       vid     death     birth
         3         2         2         2  1.000000         01.0000E+28     0.000
$#      id                                                               heading
         3Floor 3 Z
$#    nsid       dof       vad      lcid        sf       vid     death     birth
         3         3         2         2  1.000000         01.0000E+28     0.000
*BOUNDARY_SPC_SET_ID
$#      id                                                               heading
         2B_Floor 2
$#    nsid       cid      dofx      dofy      dofz     dofrx     dofry     dofrz
         2         0         1         1         1         0         0         0
$#      id                                                               heading
         4B_Top floor
$#    nsid       cid      dofx      dofy      dofz     dofrx     dofry     dofrz
         4         0         1         1         1         0         0         0
$#      id                                                               heading
         1B_Bottom floor
$#    nsid       cid      dofx      dofy      dofz     dofrx     dofry     dofrz
         1         0         1         1         1         0         0         0
$#      id                                                               heading
         6B_Facade bottom
$#    nsid       cid      dofx      dofy      dofz     dofrx     dofry     dofrz
         5         0         0         0         1         0         0         0
```

```
$
$
$
$
$$$$ LOAD BLAST ENHANCED. HERE 2.1 kg & BLAST = 1.
$
$
$
$
*LOAD_BLAST_SEGMENT_SET
$#     bid      ssid    alepid     sfnrb    scalep
         1         1         0     0.000  1.000000
*LOAD_BLAST_ENHANCED
$#     bid         m       xbo       ybo       zbo       tbo      unit     blast
         1  2.100000 615.00000-2100.0000 1032.5000     0.000         6         1
$#     cfm       cfl       cft       cfp     nidbo     death    negphs
     0.000     0.000  1.000000     0.000         01.0000E+20         0
$
$
$$$$ WEIGHT AND GRAVITY
$
$
$

*LOAD_BODY_PARTS
$#    psid
         1
*LOAD_BODY_Z
$#    lcid        sf    lciddr        xc        yc        zc       cid
         4  0.009810         0     0.000     0.000     0.000         0
*LOAD_NODE_SET
$#    nsid       dof      lcid        sf       cid        m1        m2        m3
         6         3         4 -1.200E-4         0         0         0         0
$
$
$$$$ PART COMPOSITE
$
$
$
$
*PART_COMPOSITE
$# title
Facade
$#     pid    elform      shrf      nloc     marea      hgid    adpopt  ithelfrm
         1         2     0.000     0.000     0.000         0         0         0
$#    mid1    thick1        b1    ithid1      mid2    thick2        b2    ithid2
         1  4.000000     0.000         0         2  4.000000     0.000         0
         1  4.000000     0.000         0         1  4.000000     0.000         0
         1  4.000000     0.000         0         1  4.000000     0.000         0
         1  4.000000     0.000         0         1  4.000000     0.000         0
         2  4.000000     0.000         0         1  4.000000     0.000         0
*PART_COMPOSITE
$# title
Floor 1
$#     pid    elform      shrf      nloc     marea      hgid    adpopt  ithelfrm
         2         2     0.000     0.000     0.000         0         0         0
$#    mid1    thick1        b1    ithid1      mid2    thick2        b2    ithid2
         1  4.000000     0.000         0         3  4.000000     0.000         0
         1  4.000000     0.000         0         1  4.000000     0.000         0
         1  4.000000     0.000         0         1  4.000000     0.000         0
         1  4.000000     0.000         0         1  4.000000     0.000         0
         1  4.000000     0.000         0         1  4.000000     0.000         0
```

```
*PART_COMPOSITE
$# title
Floor 2
$#     pid    elform      shrf      nloc     marea      hgid    adpopt  ithelfrm
         3         2     0.000     0.000     0.000         0         0         0
$#    mid1    thick1        b1    ithid1      mid2    thick2        b2    ithid2
         1  4.000000     0.000         0         3  4.000000     0.000         0
         1  4.000000     0.000         0         1  4.000000     0.000         0
         1  4.000000     0.000         0         1  4.000000     0.000         0
         1  4.000000     0.000         0         1  4.000000     0.000         0
         1  4.000000     0.000         0         1  4.000000     0.000         0
*PART_COMPOSITE
$# title
Floor 3
$#     pid    elform      shrf      nloc     marea      hgid    adpopt  ithelfrm
         4         2     0.000     0.000     0.000         0         0         0
$#    mid1    thick1        b1    ithid1      mid2    thick2        b2    ithid2
         1  4.000000     0.000         0         3  4.000000     0.000         0
         1  4.000000     0.000         0         1  4.000000     0.000         0
         1  4.000000     0.000         0         1  4.000000     0.000         0
         1  4.000000     0.000         0         1  4.000000     0.000         0
         1  4.000000     0.000         0         1  4.000000     0.000         0
*PART_COMPOSITE
$# title
Floor 4
$#     pid    elform      shrf      nloc     marea      hgid    adpopt  ithelfrm
         5         2     0.000     0.000     0.000         0         0         0
$#    mid1    thick1        b1    ithid1      mid2    thick2        b2    ithid2
         1  4.000000     0.000         0         3  4.000000     0.000         0
         1  4.000000     0.000         0         1  4.000000     0.000         0
         1  4.000000     0.000         0         1  4.000000     0.000         0
         1  4.000000     0.000         0         1  4.000000     0.000         0
         1  4.000000     0.000         0         1  4.000000     0.000         0
$
$
$$$$ MATERIAL
$
$
$
$

*MAT_CONCRETE_EC2_TITLE
Concrete only
$#     mid        ro        fc        ft     typec     unitc    ecuten      fcc6
         1 2.1500E-6  0.049000  0.005300  1.000000 1000.0000  0.002500     0.000
$# esoft       lchar        mu    taumxf    taumxc    ecragg     aggsz     unitl
               0.000  0.4000001.0000E+20  0.006200  0.001000     0.000  1.000000
$# ymreinf    prrinf   sureinf     typer    fracrx    fracry     lcrsu    lcalps
     0.000     0.000     0.000  1.000000     0.000     0.000         0         0
$#    aopt      et36    prt36     ecut36    lcalpc    degrad    ishchk    unlfac
     0.000     0.000  0.2500001.0000E+20         0     0.000         0  0.500000
*MAT_CONCRETE_EC2_TITLE
Reinf facade
$#     mid        ro        fc        ft     typec     unitc    ecuten      fcc6
         2 2.1500E-6  0.049000  0.005300  1.000000 1000.0000  0.002500     0.000
$# esoft       lchar        mu    taumxf    taumxc    ecragg     aggsz     unitl
               0.000  0.4000001.0000E+20  0.006200  0.001000     0.000  1.000000
$# ymreinf    prrinf   sureinf     typer    fracrx    fracry     lcrsu    lcalps
 200.00000  0.300000  0.450000  5.000000  0.015000  0.012000         3         0
$#    aopt      et36    prt36     ecut36    lcalpc    degrad    ishchk    unlfac
     0.000     0.000  0.2500001.0000E+20         0     0.000         0  0.500000
```

```
*MAT_CONCRETE_EC2_TITLE
Reinf floor
$#     mid        ro        fc        ft     typec     unitc    ecuten      fcc6
         3 2.1500E-6  0.049000  0.005300  1.000000 1000.0000  0.002500     0.000
$# esoft       lchar        mu    taumxf    taumxc    ecragg     aggsz     unitl
             0.000  0.4000001.0000E+20  1.161000  0.001000     0.000  1.000000
$# ymreinf    prrinf   sureinf     typer    fracrx    fracry     lcrsu    lcalps
 200.00000  0.300000  0.450000  5.000000  0.015000  0.016000         3         0
$#    aopt      et36    prt36     ecut36    lcalpc    degrad    ishchk    unlfac
     0.000     0.000  0.2500001.0000E+20         0     0.000         0  0.500000
$
$
$
$
$$$$ CURVES DEFINING BOUNDARY MOTION, STEEL YIELD CURVE, GRAVITATIONAL FORCE AND
$    BLAST FORCE OUTPUT
$
$
$
$
*DEFINE_CURVE_TITLE
Floor 3 xyz zero motion
$#    lcid      sidr       sfa       sfo      offa      offo    dattyp
         2         0  1.000000  1.000000     0.000     0.000         0
$#              a1                  o1
             0.000               0.000
          1000.0000               0.000
*DEFINE_CURVE_TITLE
Steel yield curve
$#    lcid      sidr       sfa       sfo      offa      offo    dattyp
         3         0  1.000000  1.000000     0.000     0.000         0
$#              a1                  o1
             0.000            1.000000
          0.220000            1.462000
          0.270000               0.000
*DEFINE_CURVE_TITLE
Gravity
$#    lcid      sidr       sfa       sfo      offa      offo    dattyp
         4         0  1.000000  1.000000     0.000     0.000         0
$#              a1                  o1
             0.000            1.000000
          1000.0000            1.000000
*DEFINE_CURVE_TITLE
Blast force
$#    lcid      sidr       sfa       sfo      offa      offo    dattyp
        10         0  1.000000  1.000000     0.000     0.000         0
$#              a1                  o1
             0.000            0.001000
          1.000000            0.010000
          7.000000            0.700000
         20.000000            1.000000
$
$ NODE INCLUDE FILES
$
*INCLUDE
nodes.k
*INCLUDE
fasad.k
*INCLUDE
bl1.k
*INCLUDE
bl2.k
*INCLUDE
bl3.k
*INCLUDE
bl4.k
*END
```